A renormalization-group analysis of the interacting resonant level model at finite bias: Generic analytic study of static properties and quench dynamics

S. Andergassen,[1] M. Pletyukhov,[1] D. Schuricht,[1] H. Schoeller,[1] and L. Borda[2,3]

[1]*Institut für Theorie der Statistischen Physik, RWTH Aachen, 52056 Aachen, Germany*
and JARA-Fundamentals of Future Information Technology
[2]*Physikalisches Institut, Universität Bonn, D-53115 Bonn, Germany*
[3]*Department of Theoretical Physics and Condensed Matter Research Group of the HAS*
TU Budapest, H-1111 Budapest, Hungary
(Dated: July 14, 2011)

Using a real-time renormalization group method we study the minimal model of a quantum dot dominated by charge fluctuations, the two-lead interacting resonant level model, at finite bias voltage. We develop a set of RG equations to treat the case of weak and strong charge fluctuations, together with the determination of power-law exponents up to second order in the Coulomb interaction. We derive analytic expressions for the charge susceptibility, the steady-state current and the conductance in the situation of arbitrary system parameters, in particular away from the particle-hole symmetric point and for asymmetric Coulomb interactions. In the generic asymmetric situation we find that power laws can be observed for the current only as function of the level position (gate voltage) but not as function of the voltage. Furthermore, we study the quench dynamics after sudden switch-on of the level-lead couplings. The time evolution of the dot occupation and current is governed by exponential relaxation accompanied by voltage-dependent oscillations and characteristic algebraic decay.

I. INTRODUCTION

The standard set-up for a quantum dot consists of a small quantum system described by a finite-dimensional Hilbert space which is coupled to several infinitely large reservoirs via energy and/or particle exchange. A difference in the chemical potentials of the reservoirs will generically lead to particle transport and thus a finite current through the dot. Here we will study the arguably simplest but non-trivial quantum dot system, namely the interacting resonant level model (IRLM). It is given by a local level coupled to two leads of non-interacting spinless fermions. The fermions can hop on and off the level. In addition, there is a Coulomb interaction between the level and the reservoirs (see Fig. 1). The IRLM constitutes the minimal model for a quantum dot dominated by charge fluctuations as spin degrees of freedom are not taken into account.

Originally the (one-lead) IRLM was introduced independently by Wiegmann and Finkelstein[1] as well as Schlottmann[2] to study the anisotropic Kondo model. They generalized earlier works by Anderson et al.[3] at the Toulouse point[4], where the Coulomb interaction between the level and the reservoir vanishes. In particular, in Refs. 1 and 2 it was shown that the IRLM and the anisotropic Kondo model possess the same partition function in the so-called long-time approximation and thus share the same universal low-temperature characteristics. Equilibrium properties like the static and dynamic susceptibilities and the relaxation rate of the IRLM have been intensively studied in the early 1980's using the Bethe Ansatz[5] as well as renormalization group (RG) techniques[6]. The equivalence between the IRLM and the

anisotropic Kondo model can be shown by bosonization and refermionization of the latter model[7].

Recently the interest in the IRLM has been revived as a minimal model to describe non-equilibrium transport through quantum dots. Initialized by the work of Mehta and Andrei[8] the model has been investigated using the Hershfield Y-operator[9], Keldysh perturbation[10] and scattering theory[11,12], field theory approaches[13–15], the numerical renormalization group method (NRG)[16] and the time-dependent density matrix renormalization group technique (TD-DMRG)[14,15]. Most of these studies were performed at the special point of particle-hole and left-right symmetry. The quantity of main interest has been the steady-state current through the resonant level. The main conclusions were that (i) at sufficiently large bias voltages a negative differential conductance appears, and that (ii) in the scaling limit, where all bare energy scales are much smaller than the bandwidth of the leads, the current decreases as a power law in the applied voltage. However, only at the self-dual point[14] it has been possible to derive closed analytic expressions for the current as a function of the applied voltage.

Recently, perturbative RG techniques in non-equilibrium[16–18] have been applied to obtain more insight into the physics of the IRLM at finite bias. In Ref. 16 a poor man scaling analysis has been performed up to next-to-leading order providing power-law exponents up to second order in the Coulomb interaction. In a non-equilibrium situation, the RG flow was cut off heuristically by the voltage which induced an emergent power-law behavior of the current as a function of the voltage. Subsequently, this analysis has been put on a more firm basis by the application of recently developed

RG methods in non-equilibrium, the functional RG[19] and the real-time RG method[20], see Ref. 21 for a recent review. A short summary of the main results of the two methods for the IRLM has been presented in Ref. 18, where a leading order expansion has been performed giving rise to power-law exponents linear in the Coulomb interaction. The results were compared to numerically exact NRG and DMRG methods and a good agreement has been observed for moderate Coulomb interactions. In particular, the conclusion was drawn that power-law behavior does not take place in the generic case of asymmetric Coulomb interactions between the dot and the left and right reservoir. In addition, the scaling behavior at resonances away from the particle-hole symmetric point has been reexamined[9]. Details of the functional RG method have been presented in Ref. 17.

In this paper we will present an extended version of Ref. 18 concerning the real-time RG method, supplemented by a generic treatment of strong charge fluctuations, a next-to-leading order analysis in the Coulomb interaction and a new result concerning power laws as function of the level position away from the particle-hole symmetric point. The real-time renormalization group in frequency space (RTRG-FS)[20] has recently been introduced in the theory of dissipative quantum systems. It provides a powerful tool in the description of non-equilibrium transport, in particular the relaxation and decoherence rates naturally arise within the proposed formalism. Previous applications to the Kondo model[22,23] in the weak coupling regime are here generalized to include charge fluctuations in strong coupling. To this end we develop RG equations, where we expand all quantities around zero Matsubara frequency, in contrast to previous treatments[22,23], where a systematic expansion around the poor man scaling solution has been performed. The RG equations are set up in a generic form, which can also be used for other models with strong charge fluctuations. In particular, for the IRLM we demonstrate that this scheme allows the study of observables close to resonances where the tunneling rate is the only relevant energy scale quantifying charge fluctuations. Furthermore, we extend the analysis in Ref. 18 by including subleading terms, which gives the exponents of power laws consistently up to second order in the Coulomb interaction. A corresponding comparison of the power-law exponent with NRG results for the charge susceptibility in equilibrium at the particle-hole symmetric point yields excellent agreement. We present approximate analytical solutions which are confirmed by numerically integrating the corresponding full RG equations and which describe the steady state as well as the quench dynamics for arbitrary system parameters. Thereby various microscopic cutoff scales of the RG flow can be identified, which is essential for the precise determination of the scaling behavior of observables. In particular, we derive closed analytic expressions for the charge susceptibility, the steady-state current and the differential conductance. We find (i) a negative differential conductance for arbitrary system pa-
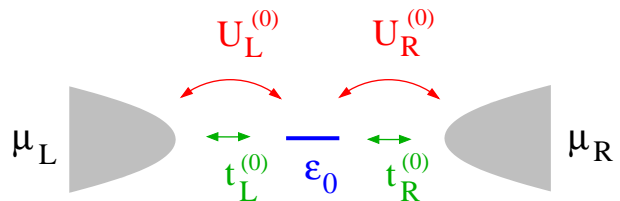

FIG. 1. (Color online) Sketch of the interacting resonant level model. A local level with energy ϵ_0 is coupled via hoppings $t_{L/R}^{(0)}$ and Coulomb couplings $U_{L/R}^{(0)}$ to two spinless fermionic reservoirs held at chemical potentials $\mu_{L/R} = \pm V/2$.

rameters, (ii) that for asymmetric Coulomb interactions the current does in general not follow a power law as a function of the bias and is recovered only in the limit of extremely large voltages, (iii) that at resonance, i.e. when the level position is aligned with one of the Fermi levels in the leads, the current does not follow a power law even in the symmetric model, and (iv) that the current or the linear conductance reveals a power law as function of the level position in the generic case, i.e. even for asymmetric Coulomb interactions and/or asymmetric tunneling couplings. The latter result was not reported in Ref. 18.

In addition, we use the analytical solution of the RG equations to study the quench dynamics in the IRLM, where we assume the couplings to the leads to be switched on suddenly. We derive closed integral representations for the resulting time evolution of the dot occupation and the current. The most notable characteristics of the time evolution of both observables are: (i) the relaxation towards the stationary values is governed by two different decay rates describing the charge relaxation on the level and its broadening induced by the coupling to the leads, respectively, (ii) the voltage appears as an important energy scale for the dynamics setting the frequency of an oscillatory behavior, and (iii) the exponential decay is accompanied by an algebraic behavior with an interaction-dependent exponent. Similar results have been obtained recently for the dynamics of the non-equilibrium Kondo model[23], showing that these features are generic.

The paper is organized as follows: In Section II we introduce the IRLM and discuss its description in Liouville space. In Section III we summarize and solve the RG equations. In Section IV we present the results for steady-state quantities as well as for the time evolution. Here we also provide a simple derivation of the appearance of the negative differential conductance. Technical details together with the generic derivation of non-equilibrium RG equations in the regime of strong charge fluctuations are reported in the Appendix.

II. MODEL

The Hamiltonian of the interacting resonant level model (IRLM) depicted in Fig. 1 is given by

$$H = H_{res} + H_D + V \ , \tag{1}$$

where

$$H_{res} = \sum_{k\alpha}(\epsilon_k + \mu_\alpha)a_{k\alpha}^\dagger a_{k\alpha} \tag{2}$$

describes a set of semi-infinite fermionic reservoirs with chemical potentials μ_α. In the case of two reservoirs $\alpha = L/R$, we choose $\mu_{L/R} = \pm V/2$. Standard second-quantized notation is used, and the energies $\epsilon_{k\alpha}$ are restricted to a finite band of width D. The dot Hamiltonian reads

$$H_D = \epsilon_0 c^\dagger c \ , \tag{3}$$

and the fermionic level is coupled to the reservoirs via

$$V = \sum_\alpha \frac{t_\alpha^{(0)}}{\sqrt{\rho_\alpha^{(0)}}}\sum_k \left(a_{k\alpha}^\dagger c + c^\dagger a_{k\alpha}\right)$$
$$+ \left(c^\dagger c - \frac{1}{2}\right)\sum_\alpha \frac{U_\alpha^{(0)}}{\rho_\alpha^{(0)}}\sum_{kk'} :a_{k\alpha}^\dagger a_{k'\alpha}: \ , \tag{4}$$

where $:\dots:$ denotes normal-ordering, and $t_\alpha^{(0)}$ and $U_\alpha^{(0)}$ are real. In the following we denote the bare parameters by the super-script $^{(0)}$. In the scaling limit the details of the frequency dependence of the local density of states in the reservoirs $\rho_\alpha(\omega)$ do not play a significant role as long as it is sufficiently regular on the energy scale of the applied voltage, which allows us to appoximate it by a constant. Following Ref. 20, we choose the Lorentzian form

$$\rho_\alpha(\omega) = \rho_\alpha^{(0)}\frac{D^2}{D^2 + \omega^2} \ . \tag{5}$$

We stress that the hybridization as well as the Coulomb interactions to the leads are allowed to be asymmetric, which corresponds to a generic setting. Furthermore, we do not restrict ourselves to the particle-hole symmetric point given by $\epsilon_0 = 0$.

We define $a_\alpha^{(\dagger)}(\omega) = \frac{1}{\sqrt{\rho_\alpha^{(0)}}}\sum_k \delta(\omega - \epsilon_k + \mu_\alpha)a_{k\alpha}^{(\dagger)}$, and introduce the vertices

$$g_{\eta\alpha} = t_\alpha^{(0)}\begin{cases} c & \text{for } \eta = + \\ c^\dagger & \text{for } \eta = - \end{cases} \tag{6}$$

and

$$g_{\eta\alpha,\eta'\alpha'} = \delta_{\eta,-\eta'}\delta_{\alpha,\alpha'}\eta\, U_\alpha^{(0)}(c^\dagger c - \frac{1}{2}) \ . \tag{7}$$

The different contributions to the Hamiltonian can then be rewritten as

$$H_{res} = \sum_\alpha \int d\omega(\omega + \mu_\alpha)a_\alpha^\dagger(\omega)a_\alpha(\omega) \ , \tag{8}$$

where we measure the energy ω of the reservoir states relative to the chemical potentials μ_α,

$$H_D = \sum_s E_s\,|s\rangle\langle s| \ , \tag{9}$$

with $s = 0, 1$, and $E_0 = 0$, $E_1 = \epsilon_0$ respectively, and

$$V = \eta \int d\omega a_1(\omega)g_1$$
$$+ \frac{1}{2}\int d\omega \int d\omega'\eta\eta':a_{1'}(\omega')a_1(\omega):g_{11'} \ , \tag{10}$$

with the multi-index $1 \equiv \eta\alpha$ containing $\eta = \pm$ for creation and annihilation operators and the lead index α. Repeated incides are assumed to be summed over. We consider the case of zero temperature throughout the manuscript since temperature is a rather trivial cutoff parameter for the RG flow, which at will can be easily incorporated in the employed RG formalism.

III. RG ANALYSIS

We will study the non-equilibrium properties of the IRLM using the real-time renormalization group method in frequency space[20] (RTRG-FS). The formalism is based on a description of the system in Liouville space. The density matrix of the full system, $\rho(t)$, is given by the solution of the von Neumann equation

$$\rho(t) = e^{-iH(t-t_0)}\rho(t_0)e^{iH(t-t_0)}$$
$$= e^{-iL(t-t_0)}\rho(t_0) \ , \tag{11}$$

where $L = [H, .]$ is the Liouvillian acting on usual operators in Hilbert space via the commutator. Initially, we assume that the density matrix is a product of an arbitrary dot part $\rho_D(t_0)$ and grandcanonical distributions for the reservoirs,

$$\rho(t_0) = \rho_D(t_0)\prod_\alpha \rho_{res}^\alpha \ . \tag{12}$$

The object of main interest is the reduced density matrix of the dot, which is obtained by tracing out the reservoir degrees of freedom

$$\rho_D(t) = \text{Tr}_{res}\,\rho(t) = \text{Tr}_{res}\,e^{-iL(t-t_0)}\rho_D(t_0)\prod_\alpha \rho_{res}^\alpha \ , \tag{13}$$

and its Laplace transform $(\text{Im}\,z > 0)$

$$\tilde{\rho}_D(z) = \int_{t_0}^\infty dt\,e^{iz(t-t_0)}\rho_D(t) = \text{Tr}_{res}\,\frac{i}{z - L}\rho(t_0) \ . \tag{14}$$

Here the Liouvillian admits the same decomposition as (1), i.e. $L = L_{res} + L_D^{(0)} + L_V$ with $L_{res} = [H_{res}, .]$, $L_D^{(0)} = [H_D, .]$, and $L_V = [V, .]$. Using the RTRG-FS we will derive the effective Liouvillian of the quantum dot

$L_D^{eff}(z)$ from which the reduced density matrix can be calculated via

$$\tilde{\rho}_D(z) = \frac{i}{z - L_D^{eff}(z)} \, \rho_D(t_0) \,. \qquad (15)$$

The stationary reduced density matrix is obtained as

$$\rho_D^{st} = \lim_{t \to \infty} \rho_D(t) = \lim_{z \to i0^+} \frac{z}{z - L_D^{eff}(z)} \, \rho_D(t_0) \,. \qquad (16)$$

The existence of a stationary density matrix was proven in Ref. 20 using the RTRG-FS as well as for the Kondo model in Ref. 24 using non-equilibrium perturbation theory to all orders. The matrix elements of the effective Liouvillian involve the rates for the processes between the two eigenstates of the dot, leading to poles of the resolvent (15) at $z_p^1 = -i\Gamma_1$ and $z_p^\pm = \pm\tilde{\epsilon} - i\Gamma_2$, where Γ_1 corresponds to the charge relaxation rate, Γ_2 describes half of the broadening of the local level, and $\tilde{\epsilon}$ is the renormalized level position.

The calculation of the current follows along the same lines. The operator for the particle current flowing from reservoir γ to the dot is defined as $I^\gamma = -dN^\gamma/dt = -i[H, N^\gamma]$, where N^γ denotes the corresponding particle number operator in lead γ. The current in lead γ then reads $\langle I^\gamma \rangle(t) = \mathrm{Tr}_D \mathrm{Tr}_{res} I^\gamma \rho(t)$. Tracing out the reservoir degrees of freedom it can be written as

$$\langle I^\gamma \rangle(z) = -i \, \mathrm{Tr}_D \, \Sigma_\gamma(z) \, \tilde{\rho}_D(z) \qquad (17)$$

in Laplace space, where $\Sigma_\gamma(z)$ denotes the current kernel to be derived below. The stationary current is given by $\langle I^\gamma \rangle^{st} = -i \, \mathrm{Tr}_D \, \Sigma_\gamma(i0^+) \, \rho_D^{st}$.

Through $L_D^{eff}(z)$, the RTRG-FS method provides direct access to the microscopic cutoff scales. By systematically integrating out the energy scales of the reservoirs step by step, a formally exact RG equation can be derived for $L_D^{eff}(z)$ as a function of a flow parameter Λ, where all reservoir energy scales beyond Λ are included. This RG equation is coupled to other RG equations for the couplings. Similar schemes can be developed for the calculation of the transport current and correlation functions[20,22]. All RG equations involve resolvents similar to the one occurring in (15), where z is shifted by the physical energy scales like the reservoirs electrochemical potentials. The cutoff scale is given by the distance to resonances, being replaced by the corresponding rate at resonance. The microscopic inclusion of decay rates as cutoff scales into non-equilibrium RG methods was also achieved within flow equation methods[25].

A. Parametrization and initial conditions

In Liouville space, defined by the basis (00 11 10 01), the bare Liouvillian is given by $L_D^{(0)} = [H_D, \cdot]$, and the bare vertices are

$$G_1^{p(0)} = \sigma^p \begin{cases} g_1 \cdot & \text{for } p = + \\ - \cdot g_1 & \text{for } p = - \end{cases} \qquad (18)$$

and

$$G_{11'}^{pp'(0)} = \delta_{pp'} \begin{cases} g_{11'} \cdot & \text{for } p = + \\ - \cdot g_{11'} & \text{for } p = - \end{cases} , \qquad (19)$$

where $\sigma^+ = \mathbb{I}$ and

$$\sigma^- = \begin{pmatrix} 1 & 0 & 0 & 0 \\ 0 & 1 & 0 & 0 \\ 0 & 0 & -1 & 0 \\ 0 & 0 & 0 & -1 \end{pmatrix} . \qquad (20)$$

The bare current vertex reads $(I^\gamma)_1^{p(0)} = -\frac{1}{2}\eta \delta_{\alpha\gamma} p \, G_1^{p(0)}$.

For the vertices the following notations are introduced:

$$\bar{G}_1^{(0)} = \sum_p G_1^{p(0)} \quad , \quad \tilde{G}_1^{(0)} = \sum_p p \, G_1^{p(0)} \quad , \qquad (21)$$

$$\bar{G}_{11'}^{(0)} = \sum_p G_{11'}^{pp(0)} \quad , \quad \tilde{G}_{11'}^{(0)} = \sum_p p \, G_{11'}^{pp(0)} \quad , \qquad (22)$$

together with $\bar{I}_1^{\gamma(0)} = \sum_p (I^\gamma)_1^{p(0)}$. We note that (21) and (22) are related to the commutators and anticommutators of (6) and (7), respectively. In matrix notation, the bare Liouvillian and the bare vertices are then given by

$$L_D^{(0)} = \epsilon_0 \begin{pmatrix} 0 & 0 & 0 & 0 \\ 0 & 0 & 0 & 0 \\ 0 & 0 & 1 & 0 \\ 0 & 0 & 0 & -1 \end{pmatrix} ,$$

$$\bar{G}_{+\alpha}^{(0)} = t_\alpha^{(0)} \begin{pmatrix} 0 & 0 & 1 & 0 \\ 0 & 0 & -1 & 0 \\ 0 & 0 & 0 & 0 \\ 1 & 1 & 0 & 0 \end{pmatrix} ,$$

$$\bar{G}_{-\alpha}^{(0)} = t_\alpha^{(0)} \begin{pmatrix} 0 & 0 & 0 & -1 \\ 0 & 0 & 0 & 1 \\ 1 & 1 & 0 & 0 \\ 0 & 0 & 0 & 0 \end{pmatrix} ,$$

$$\tilde{G}_{+\alpha}^{(0)} = t_\alpha^{(0)} \begin{pmatrix} 0 & 0 & 1 & 0 \\ 0 & 0 & 1 & 0 \\ 0 & 0 & 0 & 0 \\ -1 & 1 & 0 & 0 \end{pmatrix} ,$$

$$\tilde{G}_{-\alpha}^{(0)} = t_\alpha^{(0)} \begin{pmatrix} 0 & 0 & 0 & 1 \\ 0 & 0 & 0 & 1 \\ 1 & -1 & 0 & 0 \\ 0 & 0 & 0 & 0 \end{pmatrix} ,$$

$$\bar{G}_{+\alpha,-\alpha}^{(0)} = U_\alpha^{(0)} \begin{pmatrix} 0 & 0 & 0 & 0 \\ 0 & 0 & 0 & 0 \\ 0 & 0 & 1 & 0 \\ 0 & 0 & 0 & -1 \end{pmatrix} ,$$

$$\tilde{G}_{+\alpha,-\alpha}^{(0)} = U_\alpha^{(0)} \begin{pmatrix} -1 & 0 & 0 & 0 \\ 0 & 1 & 0 & 0 \\ 0 & 0 & 0 & 0 \\ 0 & 0 & 0 & 0 \end{pmatrix} , \qquad (23)$$

with $\bar{G}_{-\alpha,+\alpha}^{(0)} = -\bar{G}_{+\alpha,-\alpha}^{(0)}$ and $\tilde{G}_{-\alpha,+\alpha}^{(0)} = -\tilde{G}_{+\alpha,-\alpha}^{(0)}$. For the current vertex we obtain

$$\mathrm{Tr}_D \, \bar{I}_{+\alpha}^{\gamma(0)} = -\delta_{\alpha\gamma} t_\alpha^{(0)} (0 \;\; 0 \;\; 1 \;\; 0)$$

$$\mathrm{Tr}_D \, \bar{I}_{-\alpha}^{\gamma(0)} = \delta_{\alpha\gamma} t_\alpha^{(0)} (0 \;\; 0 \;\; 0 \;\; 1) \,. \qquad (24)$$

Within the RG treatment, the Liouvillian $L_D(z)$ and the vertices $\bar{G}_1(z;\omega_1)$, $\bar{G}_{11'}(z;\omega_1,\omega_1')$ and $\bar{I}_1^\gamma(z;\omega_1)$ are effective quantities, which obtain an additional dependence on the Laplace variable z and depend on frequency variables ω_1 and ω_1' (the vertices $\tilde{G}_1^{(0)}$ and $\tilde{G}_{11'}^{(0)}$ are only needed for the initial setup of the RG flow). In addition the current kernel $\Sigma_\gamma(z)$ is generated. As shown in App. A, the dependence of the vertices on the frequencies ω_1 and ω_1' can be treated in leading order by expanding around $\omega_1 = \omega_1' = 0$. Therefore, we omit it in the following and, furthermore, replace z by its real part $E \equiv \mathrm{Re}\{z\}$. The full z-dependence can be recovered finally by analytic continuation, which will be done in Sec. IV B where we study the time evolution.

Following Ref. 20, the parametrization of the renormalized quantities follows from charge conservation and the following symmetry properties

$$\mathrm{Tr}_D L_D(E) = \mathrm{Tr}_D \bar{G}_1(E) = \mathrm{Tr}_D \bar{G}_{11'}(E) = 0 \;,$$
$$L_D(E)^c = -L_D(-E) \;, \quad \Sigma_\gamma(E)^c = -\Sigma_\gamma(-E) \;,$$
$$\bar{G}_1(E)^c = -\sigma^- \bar{G}_{\bar{1}}(-E) \;, \quad \bar{G}_{11'}(E)^c = \bar{G}_{\bar{1}\bar{1}'}(-E) \;,$$
$$\bar{I}_1^\gamma(E)^c = -\sigma^- \bar{I}_{\bar{1}}(-E)^\gamma \;,$$

where $(A^c)_{s_1 s_{1'}, s_2 s_{2'}} = A^*_{s_{1'} s_1, s_{2'} s_2}$ and $\bar{1} \equiv -\eta\alpha$.

As a consequence, the renormalized Liouvillian can be written as

$$L_D(E) = \begin{pmatrix} -i\Gamma_+(E) & i\Gamma_-(E) & 0 & 0 \\ i\Gamma_+(E) & -i\Gamma_-(E) & 0 & 0 \\ 0 & 0 & \epsilon(E) & 0 \\ 0 & 0 & 0 & -\epsilon(-E)^* \end{pmatrix} , \tag{25}$$

with $\Gamma_\pm(E) = \Gamma_\pm(-E)^*$. The renormalized vertices are given by

$$\bar{G}_{+\alpha}(E) = \begin{pmatrix} 0 & 0 & t_\alpha(E) & 0 \\ 0 & 0 & -t_\alpha(E) & 0 \\ 0 & 0 & 0 & 0 \\ t_\alpha^2(E) & t_\alpha^3(E) & 0 & 0 \end{pmatrix} ,$$

$$\bar{G}_{-\alpha}(E) = \begin{pmatrix} 0 & 0 & 0 & -t_\alpha(-E)^* \\ 0 & 0 & 0 & t_\alpha(-E)^* \\ t_\alpha^2(-E)^* & t_\alpha^3(-E)^* & 0 & 0 \\ 0 & 0 & 0 & 0 \end{pmatrix} , \tag{26}$$

and

$$\bar{G}_{+\alpha,-\alpha}(E) = \begin{pmatrix} 0 & 0 & 0 & 0 \\ 0 & 0 & 0 & 0 \\ 0 & 0 & U_\alpha(E) & 0 \\ 0 & 0 & 0 & -U_\alpha(-E)^* \end{pmatrix} , \tag{27}$$

with $\bar{G}_{-\alpha,+\alpha}(E) = -\bar{G}_{+\alpha,-\alpha}(E)$. This form of $\bar{G}_{11'}(E)$ holds only in leading order, as higher-order RG contributions generate non-zero elements in the upper left 2×2 block (see Sec. III B), while the form (25) and (26) are retained to all orders. For the renormalized current vertex we obtain the parametrization

$$\mathrm{Tr}_D \bar{I}_{+\alpha}^\gamma(E) = -t_\alpha^\gamma(E) \, (0 \;\; 0 \;\; 1 \;\; 0)$$
$$\mathrm{Tr}_D \bar{I}_{-\alpha}^\gamma(E) = t_\alpha^\gamma(-E)^* \, (0 \;\; 0 \;\; 0 \;\; 1) \;, \tag{28}$$

as well as for the corresponding current kernel generated by the RG flow

$$\mathrm{Tr}_D \Sigma_\gamma(E) = i(\Gamma_\gamma^1(E) \;\; \Gamma_\gamma^2(E) \;\; 0 \;\; 0) \;, \tag{29}$$

with $\Gamma_\gamma^i(E) = \Gamma_\gamma^i(-E)^*$.

The bare values, which serve as initial conditions for the RG equations, read $\epsilon(E) = \epsilon_0$, $\Gamma_\pm(E) = 0$, $t_\alpha(E) = t_\alpha^2(E) = t_\alpha^3(E) = t_\alpha^{(0)}$, $U_\alpha(E) = U_\alpha^{(0)}$, $\Gamma_\gamma^i(E) = 0$, and $t_\alpha^\gamma(E) = \delta_{\alpha\gamma} t_\alpha^{(0)}$.

B. Flow equations

In this section we summarize the RG equations for the renormalized quantities as introduced in the previous section, a detailed derivation is given in App. A.

The diagrams taken into account are shown in Fig. 11. We consider contributions to the flow of L_D, $\bar{G}_1$ and $\bar{G}_{11'}$ to lowest order in $\Gamma \sim t^2$ to describe the scaling limit and to leading and next-to-leading order in U_α to obtain exponents up to order $O(U_\alpha^2)$. Terms of order $\sim \Gamma U_\alpha$ for $\bar{G}_{11'}$ are neglected. These would generate nonzero elements in the upper left 2×2 block of (27). For the Liouvillian and the vertices the full E-dependence crucial for the time evolution is taken into account.

Basing on the parametrization of the Liouvillian, the current kernel, and the vertices, we introduce the following definitions

$$Z(E) = \left(1 - \frac{d}{dE}\epsilon(E)\right)^{-1} \;,$$
$$\tilde{\Gamma}_\alpha(E) = 2\pi Z(E + \mu_\alpha) t_\alpha(E)^2 \;,$$
$$\Gamma_\alpha(E) = \Gamma_\alpha^1(E) - \Gamma_\alpha^2(E) \;,$$
$$\Gamma_\alpha'(E) = \frac{1}{2}\left(\Gamma_\alpha^1(E) + \Gamma_\alpha^2(E)\right) \;,$$
$$\Gamma(E) = \sum_\alpha \Gamma_\alpha(E) \;, \quad \Gamma'(E) = \sum_\alpha \Gamma_\alpha'(E) \;,$$
$$\chi(E) = Z(E)\left(E - \epsilon(E)\right) \;,$$
$$\chi'(E) = \chi(E) - 2i\gamma_0 \Lambda \ln\frac{2\Lambda - i\chi(E)}{\Lambda - i\chi(E)} \;, \tag{30}$$

where $\gamma_0 = \sum_\alpha (U_\alpha^{(0)})^2$, and Λ is a high-energy cutoff which cuts off the Matsubara frequencies of the Fermi functions of the reservoirs. Under the RG the cutoff parameter Λ flows from the initial value Λ_0 to zero. The initial cutoff is related to the physical reservoir band width D by (A55), see App. A. As shown in App. A, the flow

equations for the effective model parameters read

$$\frac{d}{d\Lambda}\tilde{\Gamma}_\alpha(E) = \tag{31}$$
$$- \left(\frac{2(U_\alpha^{(0)} - \gamma_0)}{\Lambda - i\chi'(E+\mu_\alpha)} + \frac{\gamma_0}{\Lambda - i\chi'(E+\mu_\alpha)/2} \right) \tilde{\Gamma}_\alpha(E) \,,$$

$$\frac{d}{d\Lambda}\Gamma_\alpha(E) = \tag{32}$$
$$- \frac{U_\alpha^{(0)}}{\Lambda - i\chi'(E+\mu_\alpha)}\tilde{\Gamma}_\alpha(E) + (E \to -E)^* \,,$$

$$\frac{d}{d\Lambda}\Gamma'_\alpha(E) = \tag{33}$$
$$\frac{i}{2\pi}\frac{1}{\Lambda - i\chi'(E+\mu_\alpha)}\tilde{\Gamma}_\alpha(E) + (E \to -E)^* \,,$$

$$\frac{d}{d\Lambda}\chi'(E) = \tag{34}$$
$$-i\sum_\alpha \frac{U_\alpha^{(0)}}{\Lambda + \Gamma(E-\mu_\alpha) - i(E-\mu_\alpha)}\tilde{\Gamma}_\alpha(E-\mu_\alpha) \,.$$

The remaining parameters of the Liouvillian and the vertices are given by

$$\Gamma_\pm(E) = \frac{1}{2}\Gamma(E) \pm \Gamma'(E) = \pm\sum_\alpha \Gamma_\alpha^{1/2}(E) \,, \tag{35}$$
$$t_{2/3}^\alpha(E) = t_\alpha(E)(1 \pm i\pi U_\alpha^{(0)}) \,, \tag{36}$$
$$t_\alpha^\gamma(E) = \delta_{\alpha\gamma}t_\alpha(E) \,, \tag{37}$$
$$Z(E)U_\alpha(E) = U_\alpha^{(0)} \,. \tag{38}$$

As a consequence, it turns out that $Z(E)U_\alpha(E)$ is unrenormalized up to the second order in the interaction, in agreement with previous results[16].

The initial conditions for the RG equations are $\tilde{\Gamma}_\alpha(E) = \Gamma_\alpha(E) = \Gamma_\alpha^{(0)} = 2\pi(t_\alpha^{(0)})^2$, $\Gamma'_\alpha(E) = 0$ and $\chi'(E) = E - \epsilon_0 + \frac{i}{2}\Gamma^{(0)}$, where $\Gamma^{(0)} = \sum_\alpha \Gamma_\alpha^{(0)}$. For the numerical solution of (31)-(34) a discretization in E is required, the involved numerical effort is however limited due to the fast convergence.

The RG equations (31)-(34) reduce to poor man scaling equations for large Λ, where all resolvents can be replaced by $1/\Lambda$. In this case similar power laws are obtained for the stationary current as in Ref. 16, provided that the cutoff parameter is intuitively inserted by hand. In contrast, the RG equations derived in this paper reveal microscopically the various cutoff parameters. As can be seen from (31)-(33), all rates are cut off by the distance to resonances, given by $\chi'(E+\mu_\alpha)$. On the other hand, we see from (34) that the renormalization of the level broadening, which is contained in the imaginary part of $\chi'(E)$, is cut off by $|E - \mu_\alpha - i\Gamma(E-\mu_\alpha)|$. The RG equations presented here go beyond all previous RG analysis for the IRLM. Whereas Ref. 16 provided a consistent poor man scaling analysis without a microscopic derivation of the cutoff scales, Refs. 17 and 18 showed results from a full microscopic non-equilibrium RG analysis, but only in leading order in $U_\alpha^{(0)}$ for the exponent.

C. Analytical solution

Within the RTRG-FS approach, the coupled differential equations for the flow of the effective system parameters as a function of the infrared cutoff Λ can be solved analytically. The approximate solutions are confirmed by numerically integrating the corresponding full RG equations (31)-(34).

The poor man scaling version of (31), i.e. where the resolvents are replaced by $1/\Lambda$, gives the power-law solution

$$\tilde{\Gamma}_\alpha \to \Gamma_\alpha^{(0)} (\Lambda_0/\Lambda)^{g_\alpha} \,, \tag{39}$$

with the exponent

$$g_\alpha = 2U_\alpha^{(0)} - \gamma_0 = 2U_\alpha^{(0)} - \sum_\beta (U_\beta^{(0)})^2 \,. \tag{40}$$

According to (31) this power law is cut off by $\chi'(E+\mu_\alpha)$. Therefore, the leading order solution is given by

$$\tilde{\Gamma}_\alpha(E) \simeq \Gamma_\alpha^{(0)} \left(\frac{\Lambda_0}{\Lambda - i\chi'(E+\mu_\alpha)} \right)^{g_\alpha} \,, \tag{41}$$

where the exponent is consitently calculated up to $O(U^2)$.

Since, for small $U_\alpha^{(0)} \ll 1$, the power laws lead only to a weak variation, we can use the poor man scaling solution (39) for $\tilde{\Gamma}_\alpha$ in the other RG equations (32)-(34), and read off the cutoff scale by the remaining resolvents in these equations. This gives the following leading order solution

$$\Gamma_\alpha(E) \simeq \frac{1}{2}(\tilde{\Gamma}_\alpha(E) + \tilde{\Gamma}_\alpha(-E)^*) \,, \tag{42}$$

$$\Gamma'_\alpha(E) \simeq -\frac{i}{4\pi U_\alpha^{(0)}}(\tilde{\Gamma}_\alpha(E) - \tilde{\Gamma}_\alpha(-E)^*) \,, \tag{43}$$

$$\chi'(E) \simeq E - \epsilon_0 + \frac{i}{2}\Gamma_\epsilon(E) \,, \tag{44}$$

with the renormalized level broadening

$$\Gamma_\epsilon(E) = \sum_\alpha \Gamma_\alpha^{(0)} \left(\frac{\Lambda_0}{\Lambda + \Gamma(E-\mu_\alpha) - i(E-\mu_\alpha)} \right)^{g_\alpha} \,. \tag{45}$$

We note the properties

$$\Gamma_\alpha(E)^* = \Gamma_\alpha(-E) \,, \tag{46}$$
$$\Gamma'_\alpha(E)^* = \Gamma'_\alpha(-E) \,. \tag{47}$$

In the limit $\Lambda \to 0$, we obtain

$$\Gamma_\epsilon(E) = \sum_\alpha \Gamma_\alpha^{(0)} \left(\frac{\Lambda_0}{\Gamma(E-\mu_\alpha) - i(E-\mu_\alpha)} \right)^{g_\alpha} \,, \tag{48}$$

$$\tilde{\Gamma}_\alpha(E) = \Gamma_\alpha^{(0)} \left(\frac{\Lambda_0}{\frac{1}{2}\Gamma_\epsilon(E+\mu_\alpha) - i(E+\mu_\alpha - \epsilon_0)} \right)^{g_\alpha} \,, \tag{49}$$

which, together with (42) gives a self-consistent set of equations for the determination of $\Gamma_\epsilon(E)$ and $\Gamma(E)$. In

principle this set can be solved numerically but we will provide further analytic evaluations in Section IV.

The reduced density matrix $\tilde{\rho}_D(E) = (p_0(E) \quad p_1(E) \quad 0 \quad 0)^T$ of the dot in Laplace space can be obtained from (15) and (25), with $L_D^{eff}(E) \equiv L_D(E)|_{\Lambda=0}$. After a straightforward algebra we obtain

$$p_{0/1}(E) = \frac{i}{E} p_{0/1}(t_0) + \frac{\Gamma(E) p_{0/1}(t_0) - \Gamma_{\mp}(E)}{E(E + i\Gamma(E))} , \quad (50)$$

where $p_{0/1}(t_0)$ are the initial occupation probabilities for the dot and $\Gamma_{\pm}(E) = \Gamma(E)/2 \pm \Gamma'(E)$, according to (35).

Finally, using (17) and (29), the current in Laplace space is computed using the density matrix by

$$\begin{aligned}\langle I_\alpha \rangle(E) &= -i \mathrm{Tr}_D \Sigma_\alpha(E) \tilde{\rho}_D(E) \\ &= \Gamma_\alpha^1(E) p_0(E) + \Gamma_\alpha^2(E) p_1(E) , \quad (51)\end{aligned}$$

where $\Gamma_\alpha^{1/2}(E) = \Gamma_\alpha'(E) \pm \frac{1}{2}\Gamma_\alpha(E)$, according to (30).

The stationary probabilities $p_{0/1}^{st}$ and the stationary current I^{st} follow from $p_{0/1}^{st} = \lim_{E\to 0}(-i) E\, p_{0/1}(E)$ and $I^{st} = \Gamma_\alpha^1 p_0^{st} + \Gamma_\alpha^2 p_1^{st}$, with $\Gamma_\alpha^i \equiv \Gamma_\alpha^i(E=0)$. Using (50) this gives

$$p_{0/1}^{st} = \frac{1}{2} \mp \frac{\Gamma'}{\Gamma} \quad , \quad (52)$$

$$I_\alpha^{st} = \Gamma_\alpha' - \frac{\Gamma'}{\Gamma}\Gamma_\alpha \quad , \quad (53)$$

where all rates are evaluated at $E = 0$. As required, we obtain conservation of probability $p_0^{st} + p_1^{st} = 1$ as well as current conservation $\sum_\alpha I_\alpha^{st} = 0$.

IV. RESULTS

A. Steady-state quantities

The stationary state is obtained for $E = 0$ from (52) and (53). Inserting the solution (42) and (43) for Γ_α and Γ_α' together with the expression (49) for $\tilde{\Gamma}_\alpha$, we obtain $\Gamma_\alpha = \mathrm{Re}\tilde{\Gamma}_\alpha$ and $\Gamma_\alpha' = \frac{1}{2\pi U_\alpha^{(0)}}\mathrm{Im}\tilde{\Gamma}_\alpha$, with

$$\tilde{\Gamma}_\alpha = \Gamma_\alpha^{(0)} \left(\frac{\Lambda_0}{\frac{1}{2}\Gamma_\epsilon(\mu_\alpha) - i(\mu_\alpha - \epsilon_0)} \right)^{g_\alpha} . \quad (54)$$

Since the cutoff $\Gamma_\epsilon(\mu_\alpha)$ is only relevant for $|\mu_\alpha - \epsilon_0| \sim O(\Gamma)$ and since $\Gamma_\epsilon(E)$ varies only weakly as function of E, we can replace with good accuracy $\Gamma_\epsilon(\mu_\alpha) \to \Gamma_\epsilon(\epsilon_0)$ in the last equation. Furthermore, neglecting terms with higher powers in $U_\alpha^{(0)}$, we find in leading order

$$\Gamma_\alpha \simeq \Gamma_\alpha^{(0)} \left(\frac{\Lambda_0}{|\frac{1}{2}\Gamma_\epsilon(\epsilon_0) - i(\mu_\alpha - \epsilon_0)|} \right)^{g_\alpha} , \quad (55)$$

$$\Gamma_\alpha' \simeq \frac{1}{\pi}\Gamma_\alpha \arctan \frac{\mu_\alpha - \epsilon_0}{\Gamma_\epsilon(\epsilon_0)/2} . \quad (56)$$

To determine the level broadening $\Gamma_\epsilon(\epsilon_0)$, we use (48) and replace $\Gamma(\epsilon_0 - \mu_\alpha) \to \Gamma(0) \equiv \Gamma$ in this equation by using the same arguments as above. In leading order in $U_\alpha^{(0)}$ this gives

$$\Gamma_\epsilon(\epsilon_0) \simeq \sum_\alpha \Gamma_\alpha^{(0)} \left(\frac{\Lambda_0}{|\Gamma + i(\mu_\alpha - \epsilon_0)|} \right)^{g_\alpha} . \quad (57)$$

Neglecting the factor $\frac{1}{2}$ for the cutoff parameter $\Gamma_\epsilon(\epsilon_0)$ in (55), the self-consistent solution of (57) and (55) is approximately

$$\Gamma \simeq \Gamma_\epsilon(\epsilon_0) . \quad (58)$$

Inserting (56) into (52) and (53), and using (58), we find for the stationary dot occupation $n^{st} = p_1^{st}$ and the stationary current I_α^{st}

$$n^{st} = \frac{1}{2} + \frac{1}{\pi} \sum_\alpha \frac{\Gamma_\alpha}{\Gamma} \arctan \frac{\mu_\alpha - \epsilon_0}{\Gamma/2} \quad (59)$$

$$\begin{aligned}I_\alpha^{st} = G_0 \sum_{\beta \neq \alpha} \frac{2\Gamma_\alpha \Gamma_\beta}{\Gamma} \\ \times \left(\arctan \frac{\mu_\alpha - \epsilon_0}{\Gamma/2} - \arctan \frac{\mu_\beta - \epsilon_0}{\Gamma/2} \right) , \quad (60)\end{aligned}$$

with $G_0 = \frac{e^2}{\hbar} = \frac{1}{2\pi}$ in our units. As a consequence, we find in leading order the same form as in the noninteracting case (where the result is exact) with Lorentzian resonances for the differential conductance at $\mu_\alpha = \epsilon_0$. However, the rates Γ_α entering these equations are not the bare ones but are strongly renormalized by the interaction. According to (55) and (58) they have to be determined from the self-consistent equation

$$\Gamma_\alpha \simeq \Gamma_\alpha^{(0)} \left(\frac{\Lambda_0}{|\frac{1}{2}\Gamma - i(\mu_\alpha - \epsilon_0)|} \right)^{g_\alpha} , \quad (61)$$

with $\Gamma = \sum_\alpha \Gamma_\alpha$. This equation will be further analyzed in the next section. In particular, this renormalization is responsible for a negative differential conductance at large voltage.

For simplicity, we will restrict ourselves in the following mainly to the case of two reservoirs $\alpha = L, R$ with $\mu_L = -\mu_R = V/2$. In this case the dot occupation and the current $I^{st} \equiv I_L^{st} = -I_R^{st}$ read

$$n^{st} = \frac{1}{2} + \frac{1}{\pi} \left(\frac{\Gamma_L}{\Gamma} \arctan \frac{V/2 - \epsilon_0}{\Gamma/2} - \frac{\Gamma_R}{\Gamma} \arctan \frac{V/2 + \epsilon_0}{\Gamma/2} \right) \quad (62)$$

and

$$I^{st} = G_0 \frac{2\Gamma_L \Gamma_R}{\Gamma} \left(\arctan \frac{V/2 - \epsilon_0}{\Gamma/2} + \arctan \frac{V/2 + \epsilon_0}{\Gamma/2} \right) . \quad (63)$$

1. The rates Γ_α

As outlined above the rates Γ_α are determined by the self-consistent equation (61). We define the cutoff scales

$$\Lambda_c^\alpha = \max\{|\mu_\alpha - \epsilon_0|, \frac{\Gamma}{2}\} . \qquad (64)$$

From (61) we see that Γ_α is renormalized by a power law cut off by Λ_c^α

$$\Gamma_\alpha \simeq \Gamma_\alpha^{(0)} \left(\frac{\Lambda_0}{\Lambda_c^\alpha}\right)^{g_\alpha} . \qquad (65)$$

To write this equation in terms of invariant energy scales, we introduce the strong coupling scale

$$T_K \equiv \Gamma|_{V=\epsilon_0=0} , \qquad (66)$$

and write Γ_α in the form

$$\Gamma_\alpha = T_K^\alpha \left(\frac{T_K}{\Lambda_c^\alpha}\right)^{g_\alpha} , \qquad (67)$$

with the independent scales

$$T_K^\alpha \equiv \Gamma_\alpha^{(0)} \left(\frac{\Lambda_0}{T_K}\right)^{g_\alpha} . \qquad (68)$$

The scaling limit is defined by $\Gamma_\alpha^{(0)} \to 0$ and $\Lambda_0 \to \infty$, such that T_K^α remains constant. From (65) and (66) we see that T_K is determined from the self-consistent equation

$$T_K = \sum_\alpha T_K^\alpha = \sum_\alpha \Gamma_\alpha^{(0)} \left(\frac{\Lambda_0}{T_K}\right)^{g_\alpha} \qquad (69)$$

and remains also constant in the scaling limit. For symmetric Coulomb interactions $g_\alpha = g$, we obtain the solution

$$T_K = \Gamma^{(0)} \left(\frac{\Lambda_0}{\Gamma^{(0)}}\right)^{\frac{g}{1+g}} , \quad T_K^\alpha = \frac{\Gamma_\alpha^{(0)}}{\Gamma^{(0)}} T_K , \qquad (70)$$

with $\Gamma^{(0)} = \sum_\alpha \Gamma_\alpha^{(0)}$.

In the special case of two reservoirs $\alpha = L/R$, we use in the following instead of T_K^α the invariant $T_K = T_K^L + T_K^R$ and the asymmetry parameter $c^2 = T_K^L / T_K^R$. We obtain

$$T_K^L = \frac{c^2}{1+c^2} T_K , \quad T_K^R = \frac{1}{1+c^2} T_K , \qquad (71)$$

and for symmetric Coulomb interactions

$$c = \sqrt{\frac{\Gamma_L^{(0)}}{\Gamma_R^{(0)}}} . \qquad (72)$$

T_K is the energy scale which determines the importance of charge fluctuations. Away from resonances,

where $|\mu_\alpha - \epsilon_0| \gg T_K$, charge fluctuations are weak and the RG flow of Γ_α is cut off by the scale $|\mu_\alpha - \epsilon_0|$, which describes the distance to the resonance. Close to resonances, where $|\mu_\alpha - \epsilon_0| \sim T_K$, charge fluctuations are strong, and Γ_α is cut off by T_K. Nevertheless, Γ_α is bounded by the scale T_K^α for arbitrary system parameters even for $V = \epsilon_0 = 0$, leading to finite results for all cases. Although there is no rigorous argument why our theory should be well-controlled in the presence of a single energy scale T_K, we show in the next sections that in the scaling limit our results for the charge susceptibility and the current are in excellent agreement with exact numerical methods, provided that $U_\alpha^{(0)} \ll 1$. This indicates that strong charge fluctuations are covered by our theory.

Close to resonance, where $\mu_\alpha \simeq \epsilon_0$, the rate Γ_α is logarithmically enhanced, similar to corresponding logarithmic enhancements for 2-level models with spin fluctuations (Kondo model), see Ref. 22. Defining an overall cutoff scale by $\Lambda_c = \max\{\Lambda_c^L, \Lambda_c^R\}$ and expanding in g_α, we find close to the resonance

$$\Gamma_\alpha \simeq \Gamma_\alpha^{(0)} \left(\frac{\Lambda_0}{\Lambda_c}\right)^{g_\alpha} \left(1 + g_\alpha \ln \frac{\Lambda_c}{|\mu_\alpha - \epsilon_0 + i\Gamma/2|}\right) . \quad (73)$$

In comparison to the Kondo model the IRLM is simpler in the sense that the leading order charge fluctuation processes provide a unique cutoff scale $|\mu_\alpha - \epsilon_0 + i\Gamma/2|$ for the rates. In contrast, for the Kondo model, the distance to the resonance as well as the Zeeman splitting itself serve as cutoff parameters, such that different logarithms can occur for the rates, see Ref. 22 for details.

The appearance of a negative differential conductance in the IRLM at large bias voltages (see Figs. 3 and 4) can be understood[26] very easily from the form of the rates Γ_α, while from the numerical or field-theoretical computation of the $I - V$ characteristics it is difficult to extract the physical mechanisms. In the limit $V \gg \Gamma, |\epsilon_0|$ the current (63) for two reservoirs reduces to $I^{st}(V) \simeq \frac{\Gamma_L \Gamma_R}{\Gamma}$, and to $I^{st} \simeq (\Gamma_L^{(0)} \Gamma_R^{(0)} / (\Gamma^{(0)})^2)\Gamma$ for symmetric Coulomb interactions $g_L = g_R = g$. Substituting the above expression (65) for Γ being cut off by the voltage, and using (70), we obtain

$$I^{st}(V) = \frac{\Gamma_L^{(0)} \Gamma_R^{(0)}}{\Gamma^{(0)2}} T_K \left(\frac{T_K}{V}\right)^g \sim V^{-g} , \qquad (74)$$

leading to a negative differential conductance for repulsive interactions. The power-law behavior (74) was previously obtained using a variety of other methods[9,14,17,18,26]. In contrast, Nishino et al.[12] find a critical value of $U = 2$ above which negative differential conductance appears. For attractive interactions, we obtain a power-law increase of the current as a function of voltage which is consistent with DMRG results in Ref. 14. However, we will show in Section IV A 3 that this result does no longer hold for asymmetric Coulomb interactions.

2. Charge susceptibility

The stationary charge susceptibility χ (or the static capacitance) describes the charge response of the dot due to a shift of the level position ϵ_0 and is defined by

$$\chi = -\frac{\partial n^{st}}{\partial \epsilon_0} \ . \tag{75}$$

It can be obtained directly from (59) and for arbitrary level position reads

$$\chi = \frac{1}{2\pi} \sum_\alpha \frac{\Gamma_\alpha}{(\mu_\alpha - \epsilon_0)^2 + (\frac{\Gamma}{2})^2} \ , \tag{76}$$

where we have neglected small corrections from the weak dependence of Γ_α on ϵ_0 via the power law (67). For the special case of two reservoirs with $\mu_L = -\mu_R = V/2$ and for $\epsilon_0 = 0$, this gives

$$\chi|_{\epsilon_0=0} = \frac{2}{\pi} \frac{\Gamma}{V^2 + \Gamma^2} \ . \tag{77}$$

In particular at $V = 0$, this result can be compared to exact numerical results from NRG, which are shown in Fig. 2. We obtain

$$\chi|_{\epsilon_0=V=0} = \frac{2}{\pi\Gamma|_{\epsilon_0=V=0}} = \frac{2}{\pi T_K} \ , \tag{78}$$

which can be used to define the physical scale T_K even away from the scaling limit. For symmetric Coulomb interactions $g_L = g_R = g$, we can insert T_K from (70) and get

$$\chi|_{\epsilon_0=V=0} = \frac{2}{\pi\Gamma^{(0)}} \left(\frac{\Lambda_0}{\Gamma^{(0)}} \right)^{-\frac{g}{1+g}} \ . \tag{79}$$

As can be seen from Fig. 2, the exponent agrees surprisingly well with the exact numerical result from NRG. Since $\epsilon_0 = V = 0$ is the most critical regime where strong charge fluctuations are present, this comparison strongly supports that our general solution (76) for arbitrary voltage and arbitrary level position is a very good analytical approximation to the exact result.

For $|\frac{V}{2} \pm \epsilon_0| \gg \Gamma$, power laws occur as function of V or ϵ_0. From (76), (67) and (71) we obtain

$$\chi = \frac{1}{2\pi} \frac{c}{1+c^2} T_K \tag{80}$$
$$\times \left(\frac{c}{(\frac{V}{2} - \epsilon_0)^2} \left(\frac{T_K}{|\frac{V}{2} - \epsilon_0|} \right)^{g_L} + \frac{1}{c} \frac{1}{(\frac{V}{2} + \epsilon_0)^2} \left(\frac{T_K}{|\frac{V}{2} + \epsilon_0|} \right)^{g_R} \right).$$

For the symmetric case $g_L = g_R = g$ this leads to

$$\chi = \frac{2}{\pi} \frac{1}{T_K} \left(\frac{T_K}{V} \right)^{2+g} \tag{81}$$

for $V \gg |\epsilon_0|$, and to

$$\chi = \frac{1}{2\pi} \frac{1}{T_K} \left(\frac{T_K}{|\epsilon_0|} \right)^{2+g} \tag{82}$$
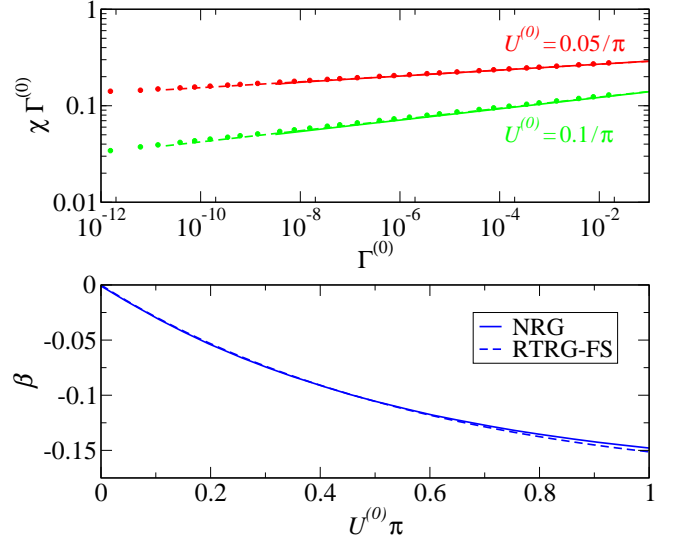

FIG. 2. (Color online) Results for the static susceptibility χ for the symmetric model with $U_L^{(0)} = U_R^{(0)} = U^{(0)}$ and $\Gamma_L^{(0)} = \Gamma_R^{(0)} = \Gamma^{(0)}$ at $\epsilon_0 = V = 0$; *upper panel:* comparison of RTRG-FS (solid lines) results, the analytic solution of the flow equations (dashed lines), and NRG data (symbols); *lower panel:* exponent $\beta = -g/(1+g)$.

for $V \ll |\epsilon_0|$.

We note that for asymmetric Coulomb interactions the general result (76) does not exhibit a clear power law if the system is coupled to more than one reservoir, neither as function of V nor of ϵ_0 nor of $\Gamma^{(0)}$. In this case, a linear combination of different power laws is involved which does not reveal a clear exponent except for if one of the energy scales is much larger than the other two.

3. Current

In the case of two reservoirs the stationary current I^{st} follows from (63). We take $\epsilon_0 > 0$ and study the off- and on-resonance case separately. A comparison of the full numerical solution of the flow equations to the analytical results obtained from (67) and (63) is provided in Fig. 3. The excellent agreement shows that for this situation already the simplified analytical treatment within poor man's scaling yields an accurate description.

The *off-resonance* case is defined by $|V/2 \pm \epsilon_0| \gg \Gamma$. Using (63) we obtain

$$I^{st} = \frac{\Gamma_L \Gamma_R}{\Gamma} \qquad \text{for} \quad \frac{V}{2} > \epsilon_0 \ , \tag{83}$$

$$I^{st} = G_0 \frac{\Gamma_L \Gamma_R}{\epsilon_0^2 - (V/2)^2} V \quad \text{for} \quad \frac{V}{2} < \epsilon_0 \ . \tag{84}$$

Inserting for the rates from (67) and (71), this gives

$$I^{st} = \frac{c}{1+c^2} T_K \frac{\left(\frac{T_K}{|V/2-\epsilon_0|} \right)^{g_L} \left(\frac{T_K}{|V/2+\epsilon_0|} \right)^{g_R}}{c \left(\frac{T_K}{|V/2-\epsilon_0|} \right)^{g_L} + \frac{1}{c} \left(\frac{T_K}{|V/2+\epsilon_0|} \right)^{g_R}} \tag{85}$$
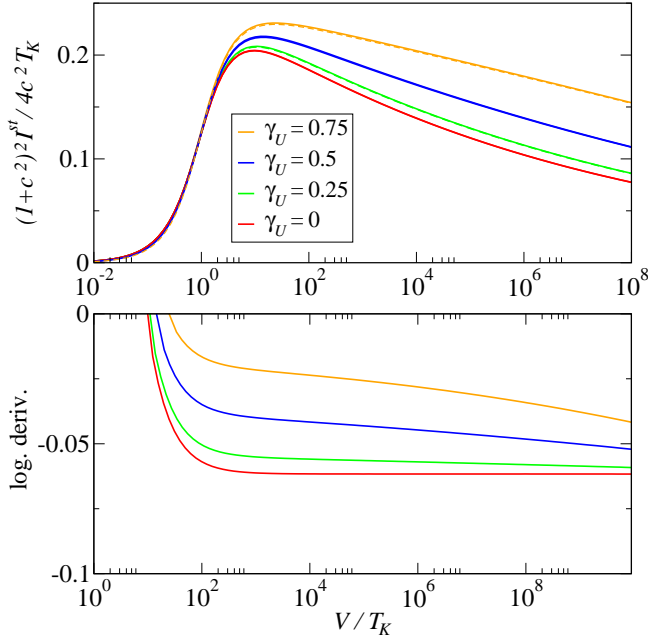
FIG. 3. (Color online) Results for the current $I(V)$ for asymmetric Coulomb interactions $U_{L/R}^{(0)} = (1 \pm \gamma_U) \, 0.1/\pi$ with $\gamma_U = 0.75$, 0.5, 0.25, 0 from top to bottom and $t_L^{(0)} = t_R^{(0)} = 0.001$, $\epsilon_0 = 0$; the numerical solution (solid lines) is compared to the analytical result (dashed lines); *lower panel:* logarithmic derivative.

for $V/2 > \epsilon_0$, and

$$I^{st} = G_0 \frac{c^2}{(1+c^2)^2} \frac{T_K^2}{\epsilon_0^2 - (V/2)^2}$$
$$\times \left(\frac{T_K}{|V/2 - \epsilon_0|} \right)^{g_L} \left(\frac{T_K}{|V/2 + \epsilon_0|} \right)^{g_R} V \quad (86)$$

for $V/2 < \epsilon_0$.

From these results one can see in what cases a power law can be expected. First, for large voltages $V \gg \epsilon_0$, a power law can only be seen for the symmetric model $g_L = g_R = g$, in which case $I^{st} \sim V^{-g}$, see Fig. 3. This is the same result obtained also in earlier studies[9,14] of the IRLM. However, in all other cases where $g_L \neq g_R$ a power law cannot be seen on realistic scales since the two terms in the denominator of Eq. (85) are typically of the same order of magnitude. The scale at which a definite power law is recovered is given by the condition $(T_K/V)^{|g_L - g_R|/2} \ll 1$ being extremely small for $|g_L - g_R| \ll 1$. In Fig. 3 the above condition is not met and the asymptotic behavior is not observed. Only if in addition to $g_L \neq g_R$ the asymmetry in the bare rates is large ($c \ll 1$ or $c \gg 1$), the power-law behavior of $I^{st}(V)$ is recovered (with exponents g_L or g_R, respectively).

Interestingly, for $V \ll \epsilon_0$, a power law also occurs in the asymmetric case, since Γ does not appear in the denominator of (86). In this case we obtain

$$I^{st} = G_0 \frac{c^2}{(1+c^2)^2} \left(\frac{T_K}{|\epsilon_0|} \right)^{2+g_L+g_R} V , \quad (87)$$
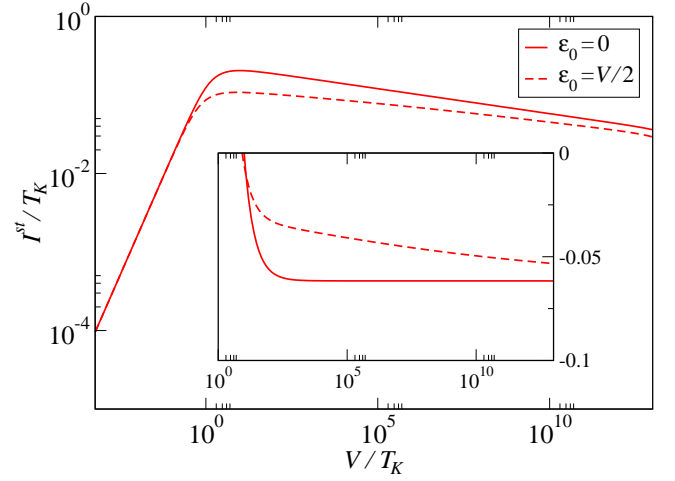

FIG. 4. (Color online) Results for the current $I(V)$ for the symmetric model with $t_L^{(0)} = t_R^{(0)} = 0.001$ and $U_L^{(0)} = U_R^{(0)} = 0.1/\pi$ off-resonance (solid lines) and on-resonance (dashed lines); *inset:* logarithmic derivative.

i.e. a power law with exponent $-(2 + g_L + g_R)$ always appears as function of the level position ϵ_0 at fixed voltage.

In the *on-resonance* case $\epsilon_0 = V/2$ the current is given by

$$I^{st} = \frac{\Gamma_L \Gamma_R}{2\Gamma} = \frac{c}{1+c^2} \frac{T_K}{2} \frac{\left(\frac{T_K}{\Gamma} \right)^{g_L} \left(\frac{T_K}{V} \right)^{g_R}}{c \left(\frac{T_K}{\Gamma} \right)^{g_L} + \frac{1}{c} \left(\frac{T_K}{V} \right)^{g_R}} . \quad (88)$$

It is important to note that if the level is in resonance with one of the reservoirs it is not in resonance with the other one. Therefore, at resonance the cutoff scales are Γ for one rate and V for the other. In contrast to the off-resonance case, no power law appears even for the left-right symmetric model, see Fig. 4. A power law is recovered only for unrealistically large V, where the second term in the last denominator of (88) can be neglected leading to $I^{st} \sim V^{-g_R}$. For the symmetric model shown in Fig. 4 the condition $(\Gamma/V)^g = 0.01 \ll 1$ is fulfilled only for $V \sim 10^{30} T_K$.

A microscopic determination of the cutoff scales is therefore essential to determine the correct on-resonance scaling behavior as a function of the voltage, which does not simply appear as an additional low-energy cutoff. The non-equilibrium physics for the generic situation $\epsilon_0 = \pm V/2$ and $g_L \neq g_R$ turns out to be more complex and can not be inferred from the linear-response behavior.

4. Conductance

Another transport property of experimental interest is the conductance $G = \frac{dI^{st}}{dV}$, which most vividly features the mentioned resonance at $\epsilon_0 = \pm V/2$ as the voltage becomes large, see Fig. 5. Analytically, the conductance
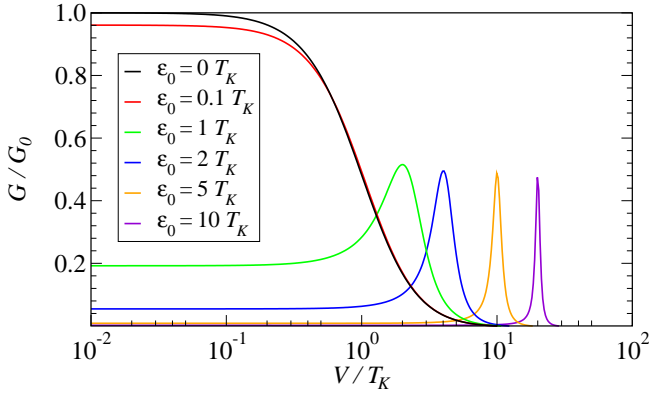
FIG. 5. (Color online) Conductance $G(V) = dI/dV$ for the symmetric model with $t_L^{(0)} = t_R^{(0)} = 0.001$, $U_L^{(0)} = U_R^{(0)} = 0.1/\pi$ and different values of the gate voltage $\epsilon_0 = 0, 0.1, 1, 2, 5, 10\,T_K$ from top to bottom.
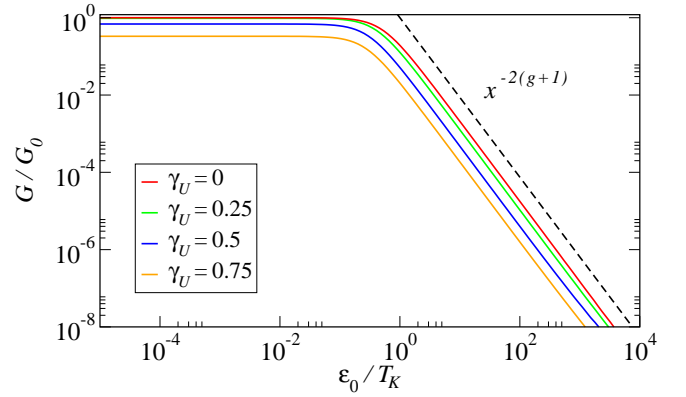

FIG. 6. (Color online) Results for the conductance $G(\epsilon_0)$ for asymmetric Coulomb interactions $U_{L/R}^{(0)} = (1 \pm \gamma_U)\,0.1/\pi$ with $\gamma_U = 0, 0.25, 0.5, 0.75$ from top to bottom and $t_L^{(0)} = t_R^{(0)} = 0.001$ at $V = 0$; the obtained power law is characterized by the exponent $\sim 2(g+1)$ in linear order, with $g = 2U^{(0)}$.

follows from differentiating (63). Neglecting small terms from the V-dependence of the rates Γ_α, we obtain

$$G = G_0 \frac{2\Gamma_L\Gamma_R}{\Gamma^2}\left(\frac{(\frac{\Gamma}{2})^2}{(\frac{V}{2}-\epsilon_0)^2+(\frac{\Gamma}{2})^2} + \frac{(\frac{\Gamma}{2})^2}{(\frac{V}{2}+\epsilon_0)^2+(\frac{\Gamma}{2})^2}\right),$$
(89)

i.e. two Lorentzian resonances at $V/2 = \pm\epsilon_0$.

For the off-resonance case $V, \Gamma \ll |\epsilon_0|$ we obtain

$$G = G_0 \frac{\Gamma_L\Gamma_R}{\epsilon_0^2} = G_0\frac{c^2}{(1+c^2)^2}\left(\frac{T_K}{|\epsilon_0|}\right)^{2+g_L+g_R}$$
(90)

in agreement with (87). Results from the solution of the full flow equations are shown in Fig. 6.

On the other hand, as a function of V the current is given by

$$I^{st} = G_0\frac{2\Gamma_L\Gamma_R}{\Gamma}\left(\pi - 2\frac{\Gamma}{V}\right)$$
(91)

for $V \gg \Gamma, |\epsilon_0|$, where we took into account the first correction to the expansion of the arctan-function in (63). Interestingly, the latter leads to an additional regime characterized by a power law independently of the asymmetry. Whereas the first term of Eq. (91) does not show a power law for asymmetric Coulomb interactions (since $\Gamma = \Gamma_L + \Gamma_R$ appears in the denominator), the second term does show a power law because Γ cancels out. Taking the derivative with respect to V, the conductance reads

$$G = G_0\left(\frac{\partial}{\partial V}\frac{2\Gamma_L\Gamma_R}{\Gamma}\right)\left(\pi - 2\frac{\Gamma}{V}\right) + G_0\frac{2\Gamma_L\Gamma_R}{\Gamma}\left(\frac{2\Gamma}{V^2}\right).$$
(92)

The derivative in the first term yields a factor $\sim g/V$ from the weak voltage dependence of the rates $\Gamma_{L/R}$, which has to be compared with the factor Γ/V^2 in the second term. Thus, for $g \ll \Gamma/V$ the second term domi-

nates and yields a power law as function of the voltage

$$G = G_0\frac{4\Gamma_L\Gamma_R}{V^2} = G_0\frac{4c^2}{(1+c^2)^2}\left(\frac{T_K}{V}\right)^{2+g_L+g_R}.$$
(93)

Thus, in contrast to the current, the conductance shows always a power law either for large voltage or for large level position with the same exponent $-(2 + g_L + g_R)$ in the range $\Gamma, |\epsilon_0| \ll V \ll \Gamma/g$.

However, for $V \gg \Gamma/g$ the first contribution in (91) dominates leading to a negative differential conductance.

B. Time evolution

The time evolution of the reduced density matrix can be obtained directly from (15) via inverse Laplace transform

$$\rho_D(t) = \frac{i}{2\pi}\int_{-\infty+i0^+}^{\infty+i0^+} dz\,\frac{e^{-izt}}{z - L_D^{eff}(z)}\,\rho_D(0),$$
(94)

where we have set the initial time to $t_0 = 0$. We recall that we assume the initial density matrix of the full system to be of the product form (12). This situation can be prepared by setting the couplings between the leads and the dot to zero for times $t < 0$. At $t = 0$ the couplings are suddenly switched on and the system evolves under the Hamiltonian (1), which results in (94) for the time evolution of the reduced density matrix. In conventional Markov approximation $L_D^{eff}(z) \approx L_D^{eff}(z = 0)$ one neglects the z-dependence of the Liouvillian, which yields simple exponential decay towards the stationary reduced density matrix. In contrast, we keep the z-dependence of the Liouvillian including its branch cuts. The time evolution of the current is obtained similarly by inverse Laplace transform of (17). This approach has previously

been used to study the real-time dynamics of the magnetization and current in the anisotropic Kondo model[23].

Specifically, using (50) we find for the occupation $n(t) = p_1(t)$ of the dot

$$n(t) = \langle c^\dagger c \rangle(t) = \big(1 + J_+(t) + J_-(t)\big)n(0) - J_+(t) \ , \quad (95)$$

where the auxiliary functions $J_\pm(t)$ are defined as

$$J_\pm(t) = \frac{1}{2\pi} \int_{-\infty+i0^+}^{\infty+i0^+} \frac{dz}{z} \frac{e^{-izt}}{z + i\Gamma(z)} \Gamma_\pm(z) \ . \quad (96)$$

Here $\Gamma_\pm(z) = \frac{1}{2}\Gamma(z) \pm \Gamma'(z)$ with $\Gamma(z) = \sum_\alpha \Gamma_\alpha(z)$ and $\Gamma'(z) = \sum_\alpha \Gamma'_\alpha(z)$ are obtained from the analytic continuation of (42), (43) and (49) (see below). Similarly, using (51) we find for the current in lead γ

$$I_\gamma(t) = \quad (97)$$

$$\frac{i}{2\pi} \int_{-\infty+i0^+}^{\infty+i0^+} \frac{dz}{z} \frac{e^{-izt}}{\Gamma(z)} \big(\Gamma_\gamma^1(z)\Gamma_-(z) + \Gamma_\gamma^2(z)\Gamma_+(z)\big)$$

$$+ \frac{i}{2\pi} \int_{-\infty+i0^+}^{\infty+i0^+} dz \frac{e^{-izt}}{\Gamma(z)} \frac{\Gamma_\gamma^1(z) - \Gamma_\gamma^2(z)}{z + i\Gamma(z)} \big(\Gamma_+(z) - n(0)\Gamma(z)\big) \ ,$$

where $\Gamma_\gamma^{1/2}(z) = \Gamma'_\gamma(z) \pm \frac{1}{2}\Gamma_\gamma(z)$.

In order to evaluate the dot occupation and the current in the interacting case we start with the analytic continuation of Eqs. (42), (43), (48) and (49). We consider the case of two reservoirs with $\mu_L = -\mu_R = V/2$ and restrict ourselves to the situation of symmetric couplings to the leads, i.e. $U_L^{(0)} = U_R^{(0)} = U^{(0)}$ and $\Gamma_L^{(0)} = \Gamma_R^{(0)} \equiv \Gamma^{(0)}/2$. In this case we can make use of the helpful identity $\Gamma_\epsilon(-E)^* = \Gamma_\epsilon(E)$, which follows from (46) and (48). As a result the analytic continuation reads

$$\Gamma_\epsilon(z) = \frac{\Gamma^{(0)}}{2} \sum_\alpha \left(\frac{\Lambda_0}{\Gamma(z - \mu_\alpha) - i(z - \mu_\alpha)} \right)^g \ , \quad (98)$$

$$\Gamma_\alpha(z) = \frac{\Gamma^{(0)}}{4} \left[\left(\frac{\Lambda_0}{\frac{1}{2}\Gamma_\epsilon(z + \mu_\alpha) - i(z + \mu_\alpha - \epsilon_0)} \right)^g \right.$$

$$\left. + \left(\frac{\Lambda_0}{\frac{1}{2}\Gamma_\epsilon(z - \mu_\alpha) - i(z - \mu_\alpha + \epsilon_0)} \right)^g \right] \ , \quad (99)$$

$$\Gamma'_\alpha(z) = -\frac{i\Gamma^{(0)}}{8\pi U^{(0)}} \left[\left(\frac{\Lambda_0}{\frac{1}{2}\Gamma_\epsilon(z + \mu_\alpha) - i(z + \mu_\alpha - \epsilon_0)} \right)^g \right.$$

$$\left. - \left(\frac{\Lambda_0}{\frac{1}{2}\Gamma_\epsilon(z - \mu_\alpha) - i(z - \mu_\alpha + \epsilon_0)} \right)^g \right] \ , \quad (100)$$

with $g = 2U^{(0)}(1 - U^{(0)})$. To proceed we first calculate the non-vanishing poles $z_1 \equiv -i\tilde{\Gamma}$ and $z_\pm \equiv \pm\tilde{\epsilon} - \frac{i}{2}\tilde{\Gamma}_\epsilon$ of the resolvent $1/(z - L_D^{eff}(z))$. Using the parameterization (25) we find $-i\Gamma(z_1) = z_1$, $\epsilon(z_+) = z_+$, and $-\epsilon(-z_-^*) = z_-^*$, which results in

$$\Gamma(-i\tilde{\Gamma}) = \tilde{\Gamma} \ , \quad \Gamma_\epsilon(\pm\tilde{\epsilon} - \frac{i}{2}\tilde{\Gamma}_\epsilon) = \tilde{\Gamma}_\epsilon \pm 2i(\tilde{\epsilon} - \epsilon_0) \ . \quad (101)$$

Second, we approximate the functions $\Gamma(z)$ and $\Gamma_\epsilon(z)$ in the denominators of (98)–(100) by their fixed points, i.e. we replace

$$\Gamma(z) \to \tilde{\Gamma} \ , \quad \Gamma_\epsilon(z) \to \tilde{\Gamma}_\epsilon \pm 2i(\tilde{\epsilon} - \epsilon_0) \ . \quad (102)$$

We use the upper (lower) approximation for $\Gamma_\epsilon(z)$ in the terms with a singularity at $z \approx \epsilon_0$ ($z \approx -\epsilon_0$). Inserting (102) we obtain

$$\Gamma_\epsilon(z) = \frac{T_K}{2} \sum_\alpha \left(\frac{T_K}{\tilde{\Gamma} - i(z - \mu_\alpha)} \right)^g \ , \quad (103)$$

$$\Gamma_\alpha(z) = \frac{T_K}{4} \left[\left(\frac{T_K}{\frac{1}{2}\tilde{\Gamma}_\epsilon - i(z + \mu_\alpha - \tilde{\epsilon})} \right)^g \right.$$

$$\left. + \left(\frac{T_K}{\frac{1}{2}\tilde{\Gamma}_\epsilon - i(z - \mu_\alpha + \tilde{\epsilon})} \right)^g \right] \ , \quad (104)$$

$$\Gamma'_\alpha(z) = -\frac{iT_K}{8\pi U^{(0)}} \left[\left(\frac{T_K}{\frac{1}{2}\tilde{\Gamma}_\epsilon - i(z + \mu_\alpha - \tilde{\epsilon})} \right)^g \right.$$

$$\left. - \left(\frac{T_K}{\frac{1}{2}\tilde{\Gamma}_\epsilon - i(z - \mu_\alpha + \tilde{\epsilon})} \right)^g \right]$$

$$\simeq -\frac{i}{2\pi}\Gamma_\alpha(z) \ln \frac{\frac{1}{2}\tilde{\Gamma}_\epsilon - i(z - \mu_\alpha + \tilde{\epsilon})}{\frac{1}{2}\tilde{\Gamma}_\epsilon - i(z + \mu_\alpha - \tilde{\epsilon})}, \quad (105)$$

where have expanded the prefactor in $\Gamma'_\alpha(z)$ up to $O(1)$ while keeping the exponents unchanged. We note that the consistent calculation of $O(U^{(0)})$ corrections of the prefactor in $\Gamma'_\alpha(z)$ requires the analysis of three-loop diagrams which is beyond the scope of our work. Furthermore we have taken the scaling limit $\Gamma^{(0)} \to 0$, $\Lambda_0 \to \infty$ with $T_K^{1+g} = \Gamma^{(0)}\Lambda_0^g$ kept constant. The decay rates $\tilde{\Gamma}$ and $\tilde{\Gamma}_\epsilon$ and the renormalized level position $\tilde{\epsilon}$ can be evaluated numerically from Eq. (101). The physical interpretation of these quantities is as follows: Whereas $\tilde{\Gamma}$ describes the charge relaxation processes on the dot and thus the relaxation of the diagonal elements of the reduced density matrix with respect to the charge states, $\tilde{\Gamma}_\epsilon$ is the broadening of the local level induced by the coupling to the leads, i.e. it characterizes the relaxation of the off-diagonal elements. Furthermore, the coupling to the leads yields a renormalization of the level position from the bare value ϵ_0 to $\tilde{\epsilon}$. For weak Coulomb interactions, $U^{(0)} \leq 0.1$, this renormalization is found to be small, $|\tilde{\epsilon}/\epsilon_0| \leq 0.01$. The approximate analytical expressions (103)–(105) show excellent agreement with the full numerical solution of the RG equations (31)-(34).

Inspecting the integral representations (96) and (97) we see that the dominant contributions stem from the singularities in the lower half-plane of the involved functions. We stress that the approximations (102) preserve this analytic structure, i.e. the poles as well as the positions and exponents of the branch cuts from the power laws remain unchanged. The integrals (96) and (97) can then be treated using standard techniques of contour integrations (see App. B). Numerical evaluation yields the
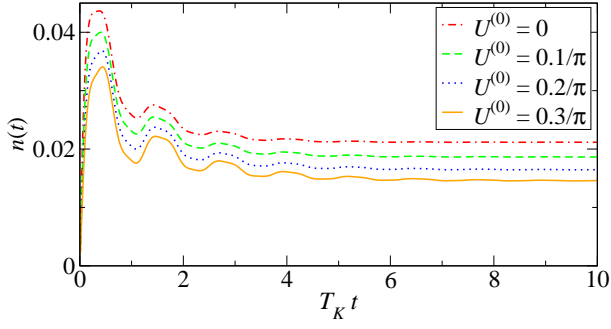
FIG. 7. (Color online) Time evolution of the dot occupation $n(t)$ for $V = \epsilon_0 = 10\,T_K$ and different values of $U^{(0)}$. The initial condition is given by $n(0) = 0$. We observe oscillating behavior at short times, $T_K t \leq 5$.

FIG. 8. (Color online) Time evolution of the dot occupation $n(t)$ for $U^{(0)} = 0.1/\pi$, $V = 100\,T_K$ and different values of ϵ_0. The initial condition is given by $n(0) = 0$.

occupation of the dot $n(t)$ as well as the current $I_L(t)$ in the left lead shown in Figs. 7–9.

Furthermore, for the long-time behavior off resonance ($|\epsilon_0 - V/2| \gg T_K, 1/t$) we are able to derive approximate analytical expressions for the dot occupation[27]

$$n(t) \approx n^{st} - \left(\frac{1}{2} + \frac{\Gamma'(-i\tilde{\Gamma})}{\tilde{\Gamma}} \right) e^{-\tilde{\Gamma}t}$$
$$+ \frac{(T_K t)^{1+g}}{2\pi} e^{-\tilde{\Gamma}_\epsilon t/2} \left[\frac{\sin\left((\tilde{\epsilon} + \frac{V}{2})t\right)}{(\tilde{\epsilon} + \frac{V}{2})^2 t^2} \right.$$
$$\left. - \pi U \frac{\cos\left((\tilde{\epsilon} + \frac{V}{2})t\right)}{(\tilde{\epsilon} + \frac{V}{2})^2 t^2} + (V \to -V) \right] \quad (106)$$

as well as for the current (we assume $V \gg T_K, 1/t$ in addition)

$$I_L(t) \approx I_L^{st} + \Gamma_L(-i\tilde{\Gamma}) \left(\frac{1}{2} + \frac{\Gamma'(-i\tilde{\Gamma})}{\tilde{\Gamma}} \right) e^{-\tilde{\Gamma}t}$$
$$+ \frac{T_K}{2\pi} (T_K t)^g e^{-\tilde{\Gamma}_\epsilon t/2} \frac{\cos\left((\tilde{\epsilon} - \frac{V}{2})t\right)}{(\tilde{\epsilon} - \frac{V}{2})t} , \quad (107)$$

with the stationary values given by (52) [or (62)] and (53), respectively. For simplicity we have considered the level to be initially empty, $n(0) = 0$. We note that in (106) the prefactor of the sine is determined up to $O(1)$ while the prefactor of the cosine has been calculated consistently up to $O(U^{(0)})$. The cosine represents the leading oscillatory behavior for $\epsilon_0 = 0$. From Figs. 7–9 as well as (106) and (107) we observe that the time evolution is governed by an exponential decay towards the stationary values, characterized by the decay rates $\tilde{\Gamma}$ and $\tilde{\Gamma}_\epsilon/2$. In addition, oscillating terms with explicitly voltage-dependent frequencies $\tilde{\epsilon} \pm V/2$ appear, accompanied by an interaction-dependent power-law decay $\sim t^{g-1}$. The last result is of particular importance for applications in error correction schemes of quantum information processing as it violates the standard assumption[28] of a purely exponential decay. The same qualitative features were observed for the time evolution in the
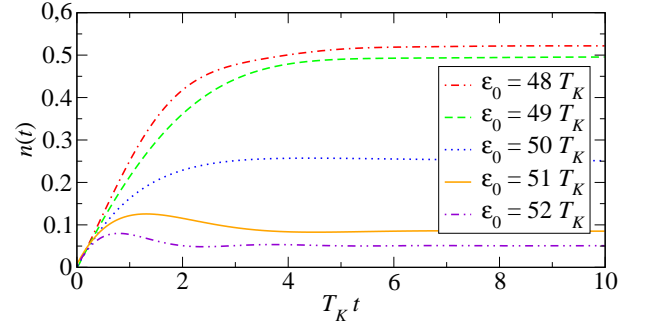
anisotropic Kondo model[23]. We stress that these qualitative features are independent of the approximations leading to (103)–(105) as they are completely determined by the analytic structure. The imaginary parts of poles and branch points lead to exponential decay, their real parts yield oscillating behavior, and the integrations along the branch cuts result in power laws.

In Fig. 9 we observe that the current starts at a non-zero value. This is due to a non-vanishing displacement current[29] $dn(t)/dt$, i.e. the fluctuating number of particles on the dot. Specifically, the particle number conservation in the full system implies

$$I_L(t) + I_R(t) = \frac{dn(t)}{dt} , \quad (108)$$

where $I_{L/R}(t) = -dN_{L/R}/dt$ is the current flowing out of lead L/R. The initial condition $n(0)$ chosen in Fig. 9 causes particles to flow from the leads to the dot as soon as the couplings $t_{L/R}^{(0)}$ are switched on. These initial currents establish on the time scale $t \sim 1/D$ with D denoting the band width, i.e. they start instantaneously in the scaling limit. The strong charge fluctuations on the dot further result in situations where particles flow off the dot into the leads even against the applied bias voltage, as can be seen by the appearance of $I_L(t) < 0$ in Fig. 9. A similar displacement current has been observed by Schmidt et al.[30] in the transient dynamics of the Anderson impurity model, where also the effects of different reservoir cut-offs have been investigated.

In the non-interacting case $U^{(0)} = 0$ the rates and the level position are simply given by $\tilde{\Gamma} = \tilde{\Gamma}_\epsilon = T_K = \Gamma^{(0)}$, and $\tilde{\epsilon} = \epsilon_0$. The contour integrals (96) and (97) can be evaluated explicitly (see App. B), resulting in

$$n(t) = e^{-T_K t} n(0) + \frac{1 - e^{-T_K t}}{2} + F_0(t) - F_1(t) \quad (109)$$

and

$$I_\gamma(t) = T_K e^{-T_K t} \frac{1 - 2n(0)}{4}$$
$$+ \frac{T_K}{2} [F_{0,\gamma}(t) - F_{0,\bar{\gamma}}(t)] + \frac{T_K}{2} F_1(t), \quad (110)$$

where $\bar{\gamma} = -\gamma$ and $F_{0/1}(t) = \sum_\alpha F_{0/1,\alpha}(t)$. The final expression for $F_{0/1,\alpha}(t)$ is given by the formula

$$F_{0/1,\alpha}(t) = \frac{e^{-T_K t/2 \pm T_K t/2}}{2\pi}\left[\pm \arctan\frac{\mu_\alpha - \epsilon_0}{T_K/2}\right.$$
$$\left. -\operatorname{Im}\operatorname{Ei}\left(\mp\frac{T_K t}{2} + i(\epsilon_0 - \mu_\alpha)t\right)\right] . \quad (111)$$

In the stationary limit $t \to \infty$ we recover from (109) and (110) the stationary values (62) and (63), respectively. In the opposite limit, at $t = 0^+$, we use the property (B9) and observe a non-zero initial value of the current

$$I_\gamma(t = 0^+) = T_K \frac{1 - 2n(0)}{4} , \quad (112)$$

i.e. the displacement current discussed above. We note that (109)–(111) contain exponentially decaying terms with rates T_K and $T_K/2$, oscillations with frequencies $\epsilon_0 \pm V/2$, and power-law behavior $\sim 1/t$.

Finally, we would like to compare our results for the non-interacting model (109)–(111) with the literature. As is well-known[31] there exists a mapping (in a certain parameter regime) between the resonant level model (and thus the anisotropic Kondo model) and the spin-boson model (or double-well problem) of dissipative quantum mechanics. By studying the time evolution in the latter, Lesage and Saleur[32] showed that generically one has to expect relaxation with various decay rates as well as oscillating terms in qualitative agreement with our results. Later Anders and Schiller[33] addressed the time evolution in the resonant level model. They derived analytic results for the dot occupation $n(t)$ in the single-lead model, which are identical to the $V \to 0$ limit of (109). They further considered quite general initial density matrices beyond the product form (12) and observed a decay with two different relaxation rates accompanied by algebraic decay as well as oscillations with frequency ϵ_0 in this more general setting as well. Komnik[34] extended their results to the two-lead model and studied the current through the system. The results he obtained are similar to (109) and (110). Furthermore, time evolution and quench dynamics in the resonant level model have been studied in the context of the anisotropic Kondo model at the Toulouse point[35].

V. CONCLUSION

We presented a non-equilibrium RG scheme to study transport properties of quantum dots in the regime of strong charge fluctuations. We developed a gauge-invariant approximation scheme to solve the RG equations analytically by expanding all quantities around zero Matsubara frequency. We illustrated the approach by a minimal and nontrivial model: the IRLM. Whereas many previous works treated the problem numerically or at the self-dual point, our analytical treatment in the
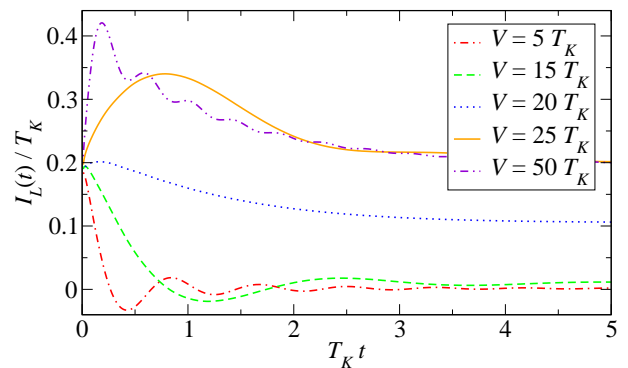

FIG. 9. (Color online) Time evolution of the current $I_L(t)$ in the left lead for $U^{(0)} = 0.1/\pi$, $\epsilon_0 = 10\,T_K$ and different values of V. The initial condition is given by $n(0) = 0$. The non-zero current at $t = 0$ is determined by the displacement current $dn(t)/dt$. The current oscillates with frequency $\sim \epsilon_0 - V/2$; note the absence of oscillations on resonance.

scaling limit and for moderate Coulomb interactions reveals the renormalized tunneling rates Γ_α parametrizing the occupation and the current in the same form as the noninteracting solution. The tunneling rates are given by a power law cut off by the distance to resonances. At resonance the total tunneling rate $\Gamma = \sum_\alpha \Gamma_\alpha$ itself is the cutoff scale leading to a self-consistent equation for Γ. We calculated the power-law exponents up to second order in the Coulomb interaction and found a very accurate agreement with NRG. Each Γ_α has its own power-law exponent $g_\alpha = 2U_\alpha^{(0)} - \sum_\beta (U_\beta^{(0)})^2$ determined by the Coulomb interaction $U_\alpha^{(0)}$ between the dot and reservoir α. As already pointed out in Ref. 18 it turned out that the current does not reveal power laws as function of the voltage in the generic case of asymmetric Coulomb interactions. The reason is that an asymmetry factor $\Gamma_L\Gamma_R/\Gamma$ occurs, which contains a linear combination of all rates in the denominator. In contrast, away from the particle-hole symmetric point, we found that power laws occur as function of the level position in the generic case, since, for large level position, only a factor $\Gamma_L\Gamma_R$ appears for the current or the linear conductance. However, the charge susceptibility shows a power law neither as function of the voltage nor of the level position in the presence of more than one reservoir, since it contains a sum of terms, each being proportional to the rate Γ_α.

Whereas the RTRG-FS scheme is limited to the scaling limit, the functional RG allows to access the steady state for arbitrary tunneling parameters beyond the scaling limit. As shown in Ref. 18, both methods provide excellent agreement in the scaling limit. The combined use of both RG approaches provides hence a complete picture of the non-equilibrium physics under consideration. As shown in this paper, an advantage of the RTRG-FS method is the analytic treatment of Coulomb interactions up to next-to-leading order, providing an excellent agreement of power-law exponents with NRG results. Further-

more, the time evolution can be studied with RTRG-FS, where we found complex relaxation dynamics similarly to previous studies of the dynamics of the non-equilibrium Kondo model[23].

The understanding of basic models of spin and charge fluctuations opens the way for applications to more complex quantum dot models. A fundamental issue for the future concerns the universality of the effects of strong charge fluctuations at resonances found for the IRLM where they induce a level broadening and a renormalization of the tunneling couplings. In particular, in the presence of both spin and charge fluctuations, as e.g. in the non-equilibrium Anderson model, the level position itself becomes renormalized and it is still an open question what the precise line shape of resonances looks like. Whereas strong charge fluctuations at resonances seem to be described by the RTRG-FS method, an open question remains whether strong spin or orbital fluctuations can be covered as well. In both cases, a single energy scale dominates the physics and cuts off the RG flow. Surprisingly, although no rigorous argument allows the truncation of the RG equations in this case, for strong charge fluctuations within the IRLM we have shown here that our results agree very accurately with exact numerical methods. Whether such an agreement holds also for strong spin and orbital fluctuations will be studied in future works.

VI. ACKNOWLEDGMENTS

Appendix A: Derivation of the RG equations

In this Section we report a detailed derivation of the flow equations and their evaluation. As outlined in detail in Ref. 20, the RG consists of two steps: The first one is a discrete step where the symmetric part of the reservoir Fermi function is integrated out, and the second step a continuous RG transformation where the Matsubara frequencies of the reservoir Fermi function are integrated out successively (note that at $T = 0$ the Matsubara frequencies are continuous). In addition to Ref. 20 we will present here a systematic treatment of the frequency dependence of the vertices, which can be quite generically used for the treatment of strong charge fluctuations. In contrast to Rfs. 20 and 22, where a systematic weak coupling expansion around the poor man scaling solution has been presented, we propose here a systematic expansion around the point where all Matsubara frequencies are set to zero. The dependence on the Laplace variable E is fully taken into account, leading to a gauge-invariant

theory. Many considerations presented here hold in general and can also be used for other models in the charge fluctuation regime. In particular, we will make use of various generic cancellations of diagrams which simplify the RG analysis considerably.

We consider a model with single and double vertices, described by the interaction (10) initially. In Liouville space the vertices are defined in (18)-(22). Following Ref. 20, we start with the discrete RG step and integrate out the symmetric part of the reservoir Fermi function by a perturbative treatment. The respective diagrams are shown in Fig. 10 and define the initial values of the second continuous RG procedure. For the initial Liouvillian we obtain

$$
\begin{aligned}
L_D(E) = {}& L_D^{(0)} - i\frac{\pi}{2}\bar{G}_1^{(0)}\tilde{G}_{\bar{1}}^{(0)} - i\frac{\pi^2}{16}D\bar{G}_{11'}^{(0)}\bar{G}_{\bar{1}'\bar{1}}^{(0)} \\
& + \frac{\pi^2}{32}\bar{G}_{11'}^{(0)}(E_{11'} - L_D^{(0)})\bar{G}_{\bar{1}'\bar{1}}^{(0)} - \frac{\pi}{4}D\bar{G}_{11'}^{(0)}\tilde{G}_{\bar{1}'\bar{1}}^{(0)} \\
& - i\frac{\pi}{4}\bar{G}_{11'}^{(0)}(E_{11'} - L_D^{(0)})\tilde{G}_{\bar{1}'\bar{1}}^{(0)} ,
\end{aligned}
\tag{A1}
$$

where we used the short-hand notation $E_{1\ldots n} = E + \bar{\mu}_1 + \cdots + \bar{\mu}_n$ with $\bar{\mu}_i = \eta_i\mu_{\alpha_i}$. The reservoir band width D is related in a certain way to the initial value Λ_0 of the continuous RG flow, see Eq. (A55) below.

The initial vertices are given by

$$
\bar{G}_1 = \bar{G}_1^{(0)} - i\frac{\pi}{2}\bar{G}_{12}^{(0)}\tilde{G}_{\bar{2}}^{(0)} - i\frac{\pi}{2}\bar{G}_2^{(0)}\tilde{G}_{\bar{2}1}^{(0)}
\tag{A2}
$$

and

$$
\bar{G}_{11'} = \bar{G}_{11'}^{(0)} - i\frac{\pi}{2}(\bar{G}_{12}^{(0)}\tilde{G}_{\bar{2}1'}^{(0)} - \bar{G}_{1'2}^{(0)}\tilde{G}_{\bar{2}1}^{(0)}) .
\tag{A3}
$$

The equations for Σ_γ and $\bar{I}_1^\gamma$ are determined analogously, the first vertex just has to be replaced by $\bar{I}_1^{\gamma(0)}$. We note that $\bar{I}_{12}^{\gamma(0)} = 0$ for our model where double vertices describe a Coulomb interaction between the dot and the reservoirs, i.e. these processes can not contribute to the current vertex. For other models, where double vertices describe spin or orbital fluctuations, $\bar{I}_{12}^{\gamma(0)}$ has to be included as well.

Inserting the form (23) of the initial matrices into above expressions and comparing with the parametrizations (25)-(29) yield the following initial values for the continuous RG flow

$$
\begin{aligned}
\Gamma_+ = {}& \Gamma_- = \frac{1}{2}\Gamma_\alpha^{(0)} , \quad \Gamma_\alpha^{(0)} = 2\pi(t_\alpha^{(0)})^2 , \\
\epsilon(E) = {}& \epsilon_0(1 - \frac{\pi^2}{16}(U_\alpha^{(0)})^2) + E\frac{\pi^2}{16}(U_\alpha^{(0)})^2 \\
& - \frac{i}{2}\Gamma_\alpha^{(0)} - i\frac{\pi^2}{8}D(U_\alpha^{(0)})^2 , \\
t_\alpha = {}& t_\alpha^{(0)} , \quad t_\alpha^\gamma = \delta_{\alpha\gamma}t_\alpha^{(0)} , \\
t_\alpha^2 = {}& t_\alpha^{(0)} - i\pi t_\alpha^{(0)}U_\alpha^{(0)} , \quad t_\alpha^3 = t_\alpha^{(0)} + i\pi t_\alpha^{(0)}U_\alpha^{(0)} , \\
\Gamma_\gamma^1 = {}& \frac{1}{2}\Gamma_\gamma^{(0)} , \quad \Gamma_\gamma^2 = -\frac{1}{2}\Gamma_\gamma^{(0)} , \\
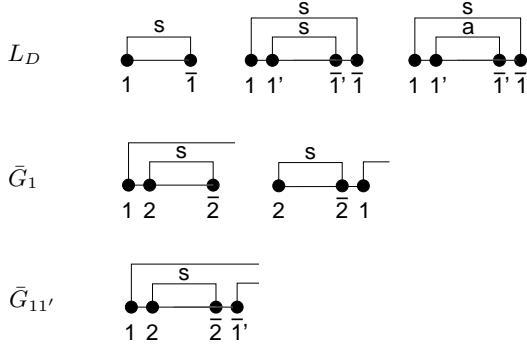U_\alpha = {}& U_\alpha^{(0)} .
\end{aligned}
\tag{A4}
$$

FIG. 10. Diagrams of the discrete RG step. Double vertices are represented by dots lying close to each other. The indices s/a refer to the symmetric/antisymmetric part of the reservoir contraction.

We proceed with the flow equations for the continuous RG procedure. The Laplace variable is decomposed into real and imaginary part as $z = E + i\omega \equiv (E,\omega)$. The Liouvillian $L_D(E,\omega)$ and the vertices $\bar{G}_1(E,\omega;\omega_1)$ and $\bar{G}_{11'}(E,\omega;\omega_1,\omega_1')$ acquire an additional dependence on the Laplace variable and on Matsubara frequencies ω_1 and ω_1'. The diagrams taken into account are shown in Fig. 11. We consider contributions to the flow of L_D, $\bar{G}_1$ and $\bar{G}_{11'}$ to lowest order in Γ and to next-to-leading order in U_α to describe the scaling limit and to obtain exponents up to order $O(U_\alpha^2)$. Terms of order $\sim \Gamma U_\alpha$ for $\bar{G}_{11'}$ are neglected. These would generate nonzero elements in the upper left 2×2 block of (27).
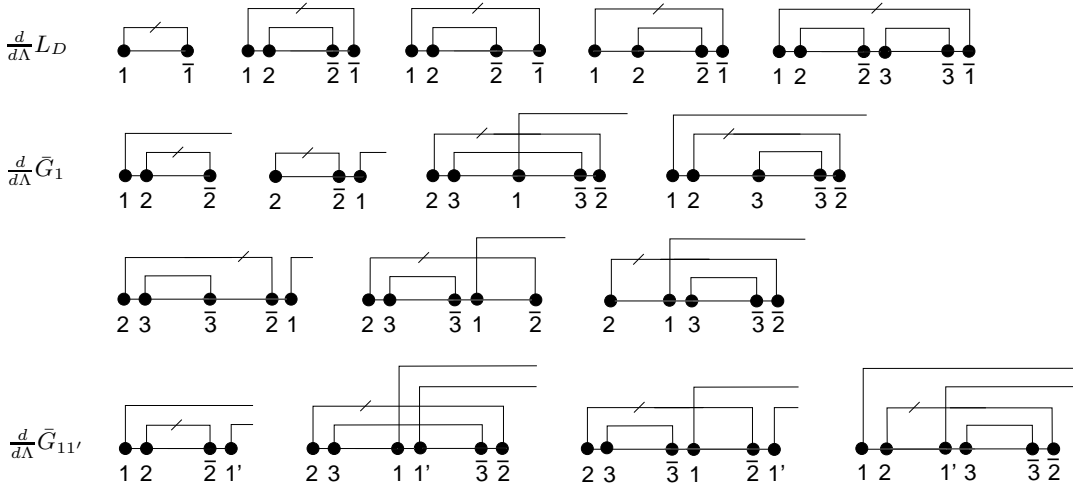

FIG. 11. Diagrams of the RG equations. Double vertices are represented by dots lying close to each other. For $\bar{G}_{11'}$ diagrams have to be subtracted where the indices 1 and $1'$ are interchanged, provided this gives a new diagram. This guarantees the relation $\bar{G}_{11'} = -\bar{G}_{1'1}$.

Using the diagrammatic rules developed in Ref. 20, the RG equations for the Liouvillian and the vertices read

$$-\frac{d}{d\Lambda}L_D(E,\omega) = -i\,\bar{G}_1(E,\omega;\Lambda)\,\Pi(E_1,\omega+\Lambda)\,\bar{G}_{\bar{1}}(E_1,\omega+\Lambda;-\Lambda)$$

$$+(-i)^2\,\bar{G}_{12}(E,\omega;\Lambda,\omega_2)\,\Pi(E_{12},\omega+\Lambda+\omega_2)\,\bar{G}_{\bar{2}\bar{1}}(E_{12},\omega+\Lambda+\omega_2;-\omega_2,-\Lambda)$$

$$+(-i)^2\,\bar{G}_{12}(E)\,\Pi(E_{12},\omega+\Lambda+\omega_2)\,\bar{G}_{\bar{2}}(E_{12})\,\Pi(E_1,\omega+\Lambda)\,\bar{G}_{\bar{1}}(E_1)$$

$$+(-i)^2\,\bar{G}_1(E)\,\Pi(E_1,\omega+\Lambda)\,\bar{G}_2(E_1)\,\Pi(E_{12},\omega+\Lambda+\omega_2)\,\bar{G}_{\bar{2}\bar{1}}(E_{12})$$

$$+(-i)^3\,\bar{G}_{12}(E)\,\Pi(E_{12},\omega+\Lambda+\omega_2)\,\bar{G}_{\bar{2}3}(E_{12})\,\Pi(E_{13},\omega+\Lambda+\omega_3)\,\bar{G}_{\bar{3}\bar{1}}(E_{13})\,, \qquad (A5)$$

$$-\frac{d}{d\Lambda}\bar{G}_1(E,\omega;\omega_1) = -i\,\bar{G}_{12}(E,\omega;\omega_1,\Lambda)\,\Pi(E_{12},\omega+\omega_1+\Lambda)\,\bar{G}_{\bar{2}}(E_{12},\omega+\omega_1+\Lambda;-\Lambda)$$

$$-i\,\bar{G}_2(E,\omega;\Lambda)\,\Pi(E_2,\omega+\Lambda)\,\bar{G}_{\bar{2}1}(E_2,\omega+\Lambda;-\Lambda,\omega_1)$$

$$+(-i)^2\,\bar{G}_{23}(E)\,\Pi(E_{23},\omega+\Lambda+\omega_3)\,\bar{G}_1(E_{23})\,\Pi(E_{123},\omega+\omega_1+\Lambda+\omega_3)\,\bar{G}_{\bar{3}\bar{2}}(E_{123})$$

$$+(-i)^2\,\bar{G}_{12}(E)\,\Pi(E_{12},\omega+\omega_1+\Lambda)\,\bar{G}_3(E_{12})\,\Pi(E_{123},\omega+\omega_1+\Lambda+\omega_3)\,\bar{G}_{\bar{3}\bar{2}}(E_{123})$$

$$+(-i)^2\,\bar{G}_{23}(E)\,\Pi(E_{23},\omega+\Lambda+\omega_3)\,\bar{G}_{\bar{3}}(E_{23})\,\Pi(E_2,\omega+\Lambda)\,\bar{G}_{\bar{2}1}(E_2)$$

$$-(-i)^2\,\bar{G}_{23}(E)\,\Pi(E_{23},\omega+\Lambda+\omega_3)\,\bar{G}_{\bar{3}1}(E_{23})\,\Pi(E_{12},\omega+\omega_1+\Lambda)\,\bar{G}_{\bar{2}}(E_{12})$$

$$-(-i)^2\,\bar{G}_2(E)\,\Pi(E_2,\omega+\Lambda)\,\bar{G}_{13}(E_2)\,\Pi(E_{123},\omega+\omega_1+\Lambda+\omega_3)\,\bar{G}_{\bar{3}\bar{2}}(E_{123})\,, \qquad (A6)$$

$$-\frac{d}{d\Lambda}\bar{G}_{11'}(E,\omega;\omega_1,\omega_1') = -i\,\bar{G}_{12}(E,\omega;\omega_1,\Lambda)\,\Pi(E_{12},\omega+\omega_1+\Lambda)\,\bar{G}_{\bar{2}1'}(E_{12},\omega+\omega_1+\Lambda;-\Lambda,\omega_1')$$

$$+i\,\bar{G}_{1'2}(E,\omega;\omega_1',\Lambda)\,\Pi(E_{1'2},\omega+\omega_1'+\Lambda)\,\bar{G}_{\bar{2}1}(E_{1'2},\omega+\omega_1'+\Lambda;-\Lambda,\omega_1)$$

$$+(-i)^2\,\bar{G}_{23}(E)\,\Pi(E_{23},\omega+\Lambda+\omega_3)\,\bar{G}_{11'}(E_{23})\,\Pi(E_{11'23},\omega+\omega_1+\omega_1'+\Lambda+\omega_3)\,\bar{G}_{\bar{3}\bar{2}}(E_{11'23})$$

$$-(-i)^2\,\bar{G}_{23}(E)\,\Pi(E_{23},\omega+\Lambda+\omega_3)\,\bar{G}_{\bar{3}1}(E_{23})\,\Pi(E_{12},\omega+\omega_1+\Lambda)\,\bar{G}_{\bar{2}1'}(E_{12})$$

$$+(-i)^2\,\bar{G}_{23}(E)\,\Pi(E_{23},\omega+\Lambda+\omega_3)\,\bar{G}_{\bar{3}1'}(E_{23})\,\Pi(E_{1'2},\omega+\omega_1'+\Lambda)\,\bar{G}_{\bar{2}1}(E_{1'2})$$

$$-(-i)^2\,\bar{G}_{12}(E)\,\Pi(E_{12},\omega+\omega_1+\Lambda)\,\bar{G}_{1'3}(E_{12})\,\Pi(E_{11'23},\omega+\omega_1+\omega_1'+\Lambda+\omega_3)\,\bar{G}_{\bar{3}\bar{2}}(E_{11'23})$$

$$+(-i)^2\,\bar{G}_{1'2}(E)\,\Pi(E_{1'2},\omega+\omega_1'+\Lambda)\,\bar{G}_{13}(E_{1'2})\,\Pi(E_{11'23},\omega+\omega_1+\omega_1'+\Lambda+\omega_3)\,\bar{G}_{\bar{3}\bar{2}}(E_{11'23})\,, \qquad (A7)$$

where

$$\Pi(E,\omega) = \frac{1}{E+i\omega-L_D(E,\omega)} \qquad (A8)$$

and

$$\bar{G}_1(E) \equiv \bar{G}_1(E,0;0)\,, \quad \bar{G}_{11'}(E) \equiv \bar{G}_{11'}(E,0;0,0)\,. \qquad (A9)$$

Implicitly, one has to sum over all indices on the r.h.s. of (A5)-(A7), which do not appear on the l.h.s. In addition, one has to perform the integral $\int_0^\Lambda d\omega_2$ and $\int_0^\Lambda d\omega_3$ at all places where the frequencies $\omega_{2/3}$ occur. The RG equations for the current kernel and the current vertex are analogous to (A5) and (A6), respectively, the only difference is that the first vertex has to be replaced by the current vertex.

Except for the real part E of the Laplace variable, all frequencies are bounded by the cutoff Λ. Since $\Lambda \to 0$ finally, it is natural to account for the dependence on the Matsubara frequencies by expanding the vertices around the reference value (A9), where all Matsubara frequencies are set to zero. Therefore, we have neglected the frequency dependence of the vertices in the higher order terms of (A5)-(A7). The frequency dependence of the vertices is calculated in leading order by neglecting the frequency dependence of the vertices on the r.h.s. of (A6) and (A7) together with omitting the higher order terms in these equations. This gives

$$\frac{d}{d\Lambda}\left\{\bar{G}_1(E,\omega;\omega_1) - \bar{G}_1(E)\right\} \simeq i\,\bar{G}_{12}(E)\,(\Pi(E_{12},\omega+\omega_1+\Lambda) - \Pi(E_{12},\Lambda))\,\bar{G}_{\bar{2}}(E_{12})$$

$$+i\,\bar{G}_2(E)\,(\Pi(E_2,\omega+\Lambda) - \Pi(E_2,\Lambda))\,\bar{G}_{\bar{2}1}(E_2)\,, \qquad (A10)$$

$$\frac{d}{d\Lambda}\left\{\bar{G}_{11'}(E,\omega;\omega_1,\omega_1') - \bar{G}_{11'}(E)\right\} \simeq i\,\bar{G}_{12}(E)\,(\Pi(E_{12},\omega+\omega_1+\Lambda) - \Pi(E_{12},\Lambda))\,\bar{G}_{\bar{2}1'}(E_{12})$$

$$-i\,\bar{G}_{1'2}(E)\,(\Pi(E_{1'2},\omega+\omega_1'+\Lambda) - \Pi(E_{1'2},\Lambda))\,\bar{G}_{\bar{2}1}(E_{1'2})\,. \qquad (A11)$$

To integrate these equations in leading order we first define a function $F(E,\omega)$ by

$$i\Pi(E,\omega) \,=\, \frac{d}{d\omega}F(E,\omega)\,. \qquad (A12)$$

Neglecting the weak logarithmic Λ-dependence of $L_D(E,\omega)$ generated by the RG (note that $\Pi(E,\omega) \equiv$ $\Pi_\Lambda(E,\omega)$ depends implicitly on Λ via $L_D(E,\omega)$), we can use

$$i\Pi(E,\omega+\Lambda) \,\simeq\, \frac{d}{d\Lambda}F(E,\omega+\Lambda)\,. \qquad (A13)$$

Using this in (A10) and (A11), and neglecting in addition the weak logarithmic Λ-dependence of the vertices generated by RG, we can integrate these equations to

$$\bar{G}_1(E,\omega;\omega_1) \simeq \bar{G}_1(E) \,+\, \bar{G}_{12}(E)\,(F(E_{12},\omega+\omega_1+\Lambda) - F(E_{12},\Lambda))\,\bar{G}_{\bar{2}}(E_{12})$$
$$+\,\bar{G}_2(E)\,(F(E_2,\omega+\Lambda)-F(E_2,\Lambda))\,\bar{G}_{\bar{2}1}(E_2)\,, \qquad (A14)$$

$$\bar{G}_{11'}(E,\omega;\omega_1,\omega_1') \simeq \bar{G}_{11'}(E) \,+\, \bar{G}_{12}(E)\,(F(E_{12},\omega+\omega_1+\Lambda) - F(E_{12},\Lambda))\,\bar{G}_{\bar{2}1'}(E_{12})$$
$$-\,\bar{G}_{1'2}(E)\,(F(E_{1'2},\omega+\omega_1'+\Lambda)-F(E_{1'2},\Lambda))\,\bar{G}_{\bar{2}1}(E_{1'2})\,. \qquad (A15)$$

To find the RG equations for $\bar{G}_1(E)$, $\bar{G}_{11'}(E)$ and

$$L_D(E) \,=\, L_D(E,0)\,, \qquad (A16)$$

we set $\omega = \omega_1 = \omega_1' = 0$ in (A5)-(A7), and insert the results (A14) and (A15) for the frequency dependence of the vertices in the lowest order terms. Furthermore, the frequency integrations can be performed by using

$$i\int_0^\Lambda d\omega\,\Pi(E,\omega+\Lambda) \,=\, K(E)\,, \qquad (A17)$$

with

$$K(E) \,=\, F(E,2\Lambda) - F(E,\Lambda)\,. \qquad (A18)$$

Collecting the various terms one finds after some straightforward algebra

$$\frac{d}{d\Lambda}L_D(E) \,=\, i\,\bar{G}_1(E)\,\Pi(E_1,\Lambda)\,\bar{G}_{\bar{1}}(E_1) \,-\, i\,\bar{G}_{12}(E)\,K(E_{12})\,\bar{G}_{\bar{2}\bar{1}}(E_{12})$$
$$-\,2i\,\bar{G}_{12}(E)\,K(E_{12})\,\bar{G}_{\bar{2}3}(E_{12})\,K(E_{13})\,\bar{G}_{\bar{3}\bar{1}}(E_{13})\,, \qquad (A19)$$

$$\frac{d}{d\Lambda}\bar{G}_1(E) \,=\, i\,\bar{G}_{12}(E)\,\Pi(E_{12},\Lambda)\,\bar{G}_{\bar{2}}(E_{12}) \,+\, i\,\bar{G}_2(E)\,\Pi(E_2,\Lambda)\,\bar{G}_{\bar{2}1}(E_2)$$
$$+\,\bar{G}_{23}(E)\,\Pi(E_{23},\Lambda+\omega_3)\,\bar{G}_1(E_{23})\,\Pi(E_{123},\Lambda+\omega_3)\,\bar{G}_{\bar{3}\bar{2}}(E_{123})\,, \qquad (A20)$$

$$\frac{d}{d\Lambda}\bar{G}_{11'}(E) \,=\, i\,\bar{G}_{12}(E)\,\Pi(E_{12},\Lambda)\,\bar{G}_{\bar{2}1'}(E_{12}) \,-\, i\,\bar{G}_{1'2}(E)\,\Pi(E_{1'2},\Lambda)\,\bar{G}_{\bar{2}1}(E_{1'2})$$
$$+\,\bar{G}_{23}(E)\,\Pi(E_{23},\Lambda+\omega_3)\,\bar{G}_{11'}(E_{23})\,\Pi(E_{11'23},\Lambda+\omega_3)\,\bar{G}_{\bar{3}\bar{2}}(E_{11'23})\,. \qquad (A21)$$

It turns out that many generic cancellations occur. In particular the corrections from the frequency dependence of the vertices from the lowest order terms cancel with corresponding diagrams in higher orders. For $\bar{G}_1(E)$ ($\bar{G}_{11'}(E)$) only the first three (two) diagrams of Fig. 11 remain with frequency independent vertices. For $L_D(E)$ the cancellation is not complete but the third and fourth diagrams cancel against frequency dependent corrections of the first two diagrams, whereas the last diagram obtains a factor 2. These cancellations simplify the RG analysis considerably and appear to be a generic model-independent feature.

To calculate the remaining frequency integrations in (A20) and (A21), and to find explicit representations for $\Pi(E,\omega)$, $F(E)$ and $K(E)$, we first introduce the spectral decomposition of the Liouvillian

$$L_D(E,\omega) \,=\, \sum_i \lambda_i(E,\omega)\,P_i(E,\omega)\,. \qquad (A22)$$

Here, λ_i denote the eigenvalues of the Liouvillian and

P_i the projectors onto the eigenstates (note that the Liouvillian is non-hermitian, so that the eigenvalues are complex valued, and the right and left eigenvectors are not identical). (A22) leads to a corresponding spectral representation of the resolvent $\Pi(E,\omega)$, defined in (A8). In leading order, we again expand in ω up to first order for the eigenvalues $\lambda_i(E,\omega)$, whereas we neglect the ω-dependence of the projectors $P_i(E,\omega)$. This leads to the approximation

$$\Pi(E,\omega) \simeq -i \sum_i \frac{Z_i(E)}{\omega - i\chi_i(E)} P_i(E) , \qquad (A23)$$

where we defined the Z-factor

$$Z_i(E) = \frac{1}{1 - \frac{d}{dE}\lambda_i(E)} \qquad (A24)$$

and the distance to the resonant positions

$$\chi_i(E) = Z_i(E)(E - \lambda_i(E)) . \qquad (A25)$$

Here, $\lambda_i(E) \equiv \lambda_i(E,0)$ and $P_i(E) \equiv P_i(E,0)$. Within this approximation we obtain

$$F(E,\omega) \simeq \sum_i Z_i(E) \ln(\omega - i\chi_i(E))P_i(E) , \qquad (A26)$$

$$K(E) \simeq \sum_i Z_i(E) \ln\left(\frac{2\Lambda - i\chi_i(E)}{\Lambda - i\chi_i(E)}\right) P_i(E) . \qquad (A27)$$

The set of RG equations (A19)-(A21) is thus complete and can be solved for a specific model. In particular, it turns out that our approximations are gauge-invariant, i.e. if all single-particle levels of the dot, all chemical potentials of the reservoirs and the Laplace variable E are shifted by the same amount, all physical observables remain the same. This is only the case if the E-dependence of all quantities is fully taken into account, an expansion

around a fixed value of E, like e.g. $E = 0$, would not lead to a gauge-invariant theory.

We now turn to the evaluation of the RG equations for the IRLM. Using the form (25) for the Liouvillian, the eigenvalues are given by

$$\lambda_0(E) = 0 , \quad \lambda_1(E) = -i\Gamma(E) ,$$
$$\lambda_+(E) = \epsilon(E) , \quad \lambda_-(E) = -\epsilon(-E)^* , \quad (A28)$$

with the corresponding projectors

$$P_0(E) = \frac{1}{\Gamma(E)} \begin{pmatrix} \Gamma_-(E) & \Gamma_-(E) & 0 & 0 \\ \Gamma_+(E) & \Gamma_+(E) & 0 & 0 \\ 0 & 0 & 0 & 0 \\ 0 & 0 & 0 & 0 \end{pmatrix} ,$$

$$P_1(E) = \frac{1}{\Gamma(E)} \begin{pmatrix} \Gamma_+(E) & -\Gamma_-(E) & 0 & 0 \\ -\Gamma_+(E) & \Gamma_-(E) & 0 & 0 \\ 0 & 0 & 0 & 0 \\ 0 & 0 & 0 & 0 \end{pmatrix} ,$$

$$P_+(E) = \begin{pmatrix} 0 & 0 & 0 & 0 \\ 0 & 0 & 0 & 0 \\ 0 & 0 & 1 & 0 \\ 0 & 0 & 0 & 0 \end{pmatrix} , \quad P_-(E) = \begin{pmatrix} 0 & 0 & 0 & 0 \\ 0 & 0 & 0 & 0 \\ 0 & 0 & 0 & 0 \\ 0 & 0 & 0 & 1 \end{pmatrix} .$$

$$(A29)$$

Using $\Gamma(E) = \Gamma(-E)^*$, we obtain for the Z-factors and the χ-functions

$$Z_1(E) = Z_1(-E)^* = (1 + i\frac{d}{dE}\Gamma(E))^{-1} , \qquad (A30)$$

$$\chi_1(E) = -\chi_1(-E)^* = Z_1(E)(E + i\Gamma(E)) , \qquad (A31)$$

$$Z(E) \equiv Z_+(E) = Z_-(-E)^* = (1 - \frac{d}{dE}\epsilon(E))^{-1} , \quad (A32)$$

$$\chi(E) \equiv \chi_+(E) = \chi_-(-E)^* = Z(E)(E - \epsilon(E)) . \quad (A33)$$

Summing over η and taking into account $\bar{G}_{+\alpha,-\alpha}(E) = -\bar{G}_{-\alpha,+\alpha}(E)$, the flow equations (A19)-(A21) can be simplified to

$$\frac{d}{d\Lambda}L_D(E) = i\bar{G}_{+\alpha}(E)\Pi(E + \mu_\alpha, \Lambda)\bar{G}_{-\alpha}(E + \mu_\alpha) + i\bar{G}_{-\alpha}(E)\Pi(E - \mu_\alpha, \Lambda)\bar{G}_{+\alpha}(E - \mu_\alpha)$$

$$- 2i\bar{G}_{+\alpha,-\alpha}(E)K(E)\bar{G}_{+\alpha,-\alpha}(E) , \qquad (A34)$$

$$\frac{d}{d\Lambda}\bar{G}_{+\alpha}(E) = i\bar{G}_{+\alpha,-\alpha}(E)\Pi(E, \Lambda)\bar{G}_{+\alpha}(E) - i\bar{G}_{+\alpha}(E)\Pi(E + \mu_\alpha, \Lambda)\bar{G}_{+\alpha,-\alpha}(E + \mu_\alpha) , \qquad (A35)$$

$$\frac{d}{d\Lambda}\bar{G}_{+\alpha,-\alpha}(E) = 2\bar{G}_{+\alpha',-\alpha'}(E)\Pi(E, \Lambda + \omega_3)\bar{G}_{+\alpha,-\alpha}(E)\Pi(E, \Lambda + \omega_3)\bar{G}_{+\alpha',-\alpha'}(E) . \qquad (A36)$$

The RG equations for the current kernel and vertex read

$$\frac{d}{d\Lambda}\Sigma_\gamma(E) = i\bar{I}^\gamma_{+\alpha}(E)\Pi(E + \mu_\alpha + i\Lambda)\bar{G}_{-\alpha}(E + \mu_\alpha)$$

$$+ i\bar{I}^\gamma_{-\alpha}(E)\Pi(E - \mu_\alpha + i\Lambda)\bar{G}_{+\alpha}(E - \mu_\alpha) ,$$

$$\frac{d}{d\Lambda}\bar{I}^\gamma_{+\alpha}(E) = -i\bar{I}^\gamma_{+\alpha}(E)\Pi(E + \mu_\alpha + i\Lambda)\bar{G}_{+\alpha,-\alpha}(E + \mu_\alpha) ,$$

$$\frac{d}{d\Lambda}\bar{I}^\gamma_{-\alpha}(E) = i\bar{I}^\gamma_{-\alpha}(E)\Pi(E - \mu_\alpha + i\Lambda)\bar{G}_{+\alpha,-\alpha}(E + \mu_\alpha) .$$

$$(A37)$$

For the derivation of the explicit flow equations for the effective parameters as introduced in the matrix representations of the Liouvillian and the vertices we use the

following helpful identities:

$$\bar{G}_{\eta\alpha}P_{-\eta} = P_{\eta}\bar{G}_{\eta\alpha} = 0 \ ,$$
$$\bar{G}_{+\alpha,-\alpha'}P_1 = P_1\bar{G}_{+\alpha,-\alpha} = 0 \ ,$$
$$P_+\bar{G}_{-\alpha}P_- = P_-\bar{G}_{+\alpha}P_+ = 0 \ ,$$
$$\bar{G}_{12}P_i\bar{G}_3P_j\bar{G}_{45} = 0 \quad \text{for} \quad i,j = 1,\pm \ ,$$
$$\bar{G}_{+\alpha}(E)P_1(E_1)\bar{G}_{-\alpha'} = -(t_\alpha^2 - t_\alpha^3)(E)t_1^{\alpha'}(-E')^*P_- \ ,$$
$$\bar{G}_{-\alpha}(E)P_1(E_1)\bar{G}_{+\alpha'} = (t_\alpha^2 - t_\alpha^3)(-E)^*t_1^{\alpha'}(-E')P_+ \ ,$$
$$\bar{G}_{+\alpha,-\alpha'}(E)P_+ = P_+\bar{G}_{+\alpha,-\alpha}(E) = U_\alpha(E)P_+ \ ,$$
$$\bar{G}_{+\alpha,-\alpha'}(E)P_- = P_+\bar{G}_{+\alpha,-\alpha}(E) = -U_\alpha(-E)^*P_- \ ,$$
$$\text{(A38)}$$

and

$$\bar{G}_{+\alpha}(E)P_+(E_1)\bar{G}_{-\alpha'}(E') =$$
$$t_\alpha(E)\begin{pmatrix} t_\alpha^2(-E')^* & t_\alpha^3(-E')^* & 0 & 0 \\ -t_\alpha^2(-E')^* & -t_\alpha^3(-E')^* & 0 & 0 \\ 0 & 0 & 0 & 0 \\ 0 & 0 & 0 & 0 \end{pmatrix} \ , \quad \text{(A39)}$$

with

$$\bar{G}_{+\alpha}(E)P_+(E_1)\bar{G}_{-\alpha'}(E') = -\bar{G}_{-\alpha}(-E)^*P_-\bar{G}_\alpha(-E')^* \ . \quad \text{(A40)}$$

Using Eqs. (A23) and (A27), the explicit flow equations for the rates $\Gamma_\pm(E)$ and the level position $\epsilon(E)$ are determined from the above Eq. (A34) for L_D and its parametrization (25) to

$$\frac{d}{d\Lambda}\Gamma_\pm(E) = \pm i \sum_\alpha \frac{Z(E+\mu_\alpha)}{\Lambda - i\chi(E+\mu_\alpha)} t_\alpha(E) t_{2/3}^\alpha(-E-\mu_\alpha)^*$$
$$+ (E \to -E)^* \ , \quad \text{(A41)}$$

$$\frac{d}{d\Lambda}\epsilon(E) = \sum_\alpha \frac{Z_1(E-\mu_\alpha)}{\Lambda - i\chi_1(E-\mu_\alpha)} t_\alpha(E-\mu_\alpha)t_\alpha'(E-\mu_\alpha)$$
$$- 2iZ(E)\gamma(E)\ln\frac{2\Lambda - i\chi(E)}{\Lambda - i\chi(E)} \ , \quad \text{(A42)}$$

with $\gamma(E) = \sum_\alpha U_\alpha(E)^2$ and $t_\alpha'(E) = t_\alpha^2(-E-\mu_\alpha)^* - t_\alpha^3(-E-\mu_\alpha)^*$. Similarly Eq. (A35) is evaluated using matrix (26) to

$$\frac{d}{d\Lambda}t_\alpha(E) = -\frac{Z(E+\mu_\alpha)}{\Lambda - i\chi(E+\mu_\alpha)} U_\alpha(E+\mu_\alpha)t_\alpha(E) \ ,$$
$$\frac{d}{d\Lambda}t_\alpha^{2/3}(E) = -\frac{Z(-E)^*}{\Lambda + i\chi(-E)^*} U_\alpha(-E)^*t_\alpha^{2/3}(E) \ ,$$

which yields

$$t_\alpha(E) = \frac{1}{2}[t_\alpha^2(-E-\mu_\alpha)^* + t_\alpha^3(-E-\mu_\alpha)^*] \ ,$$
$$t_\alpha'(E) = t_\alpha^2(-E-\mu_\alpha)^* - t_\alpha^3(-E-\mu_\alpha)^* = 2\pi i U_\alpha^{(0)}t_\alpha(E) \ ,$$

since the corresponding flow equations have the same form and the initial conditions are equal. As a consequence, introducing the rates $\Gamma(E) = \Gamma_+(E) + \Gamma_-(E)$

and $\Gamma'(E) = (\Gamma_+(E) - \Gamma_-(E))/2$, the flow equations for the two rates can be expressed in terms of the single hopping variable $t_\alpha(E)$. The flow equation for U_α is obtained by using Eq. (27) and integrating Eq. (A36) over ω_3

$$\frac{d}{d\Lambda}U_\alpha(E) = -\frac{2\Lambda Z(E)^2}{(\Lambda - i\chi(E))(2\Lambda - i\chi(E))}U_\alpha(E)\gamma(E) \ . \quad \text{(A43)}$$

Eqs. (28) and (29), together with the RG equation for the Liouvillian (A34), yield

$$\frac{d}{d\Lambda}t_\alpha^\gamma(E) = -\frac{Z(E+\mu_\alpha)}{\Lambda - i\chi(E+\mu_\alpha)}U_\alpha(E+\mu_\alpha)t_\alpha^\gamma(E)$$

for the current hopping amplitude, and

$$\frac{d}{d\Lambda}\Gamma_\gamma^{1/2}(E) = i\sum_\alpha \frac{Z(E+\mu_\alpha)}{\Lambda - i\chi(E+\mu_\alpha)}t_\alpha^\gamma(E)t_\alpha^{2/3}(-E-\mu_\alpha)^*$$
$$+ (E \to -E)^*$$

for the current rates. Comparing with the equations for $t_\alpha(E)$ and $\Gamma_\pm(E)$ and considering the respective initial conditions of Sec. III B it follows

$$t_\alpha^\gamma(E) = \delta_{\alpha\gamma}t_\alpha(E) \ , \quad \Gamma_\pm(E) = \pm\sum_\alpha \Gamma_\alpha^{1/2}(E) \ . \quad \text{(A44)}$$

Summarizing, the flow equations for the effective model parameters read

$$\frac{d}{d\Lambda}\Gamma_\alpha(E) = -2\pi\frac{Z(E+\mu_\alpha)}{\Lambda - i\chi(E+\mu_\alpha)}U_\alpha^{(0)}t_\alpha(E)^2$$
$$- (E \to -E)^* \ ,$$
$$\frac{d}{d\Lambda}\Gamma_\alpha'(E) = i\frac{Z(E+\mu_\alpha)}{\Lambda - i\chi(E+\mu_\alpha)}t_\alpha(E)^2 + (E \to -E)^* \ ,$$
$$\frac{d}{d\Lambda}t_\alpha(E) = -\frac{Z(E+\mu_\alpha)}{\Lambda - i\chi(E+\mu_\alpha)}U_\alpha(E+\mu_\alpha)t_\alpha(E) \ ,$$
$$\frac{d}{d\Lambda}\epsilon(E) = 2\pi i\sum_\alpha \frac{Z_1(E-\mu_\alpha)}{\Lambda - i\chi_1(E-\mu_\alpha)}U_\alpha^{(0)}t_\alpha(E-\mu_\alpha)^2$$
$$- 2iZ(E)\gamma(E)\ln\frac{2\Lambda - i\chi(E)}{\Lambda - i\chi(E)} \ ,$$
$$\frac{d}{d\Lambda}U_\alpha(E) = -\frac{2\Lambda Z(E)^2}{(\Lambda - i\chi(E))(2\Lambda - i\chi(E))}U_\alpha(E)\gamma(E) \ ,$$
$$\text{(A45)}$$

where we introduced the rates $\Gamma_\alpha(E) = \Gamma_\alpha^1(E) - \Gamma_\alpha^2(E)$ and $\Gamma_\alpha'(E) = (1/2)(\Gamma_\alpha^1(E) + \Gamma_\alpha^2(E))$, according to the definitions (30).

We now determine and discuss the equations for the Z-factors $Z(E)$ and $Z_1(E)$, and subsequently for $\chi(E)$ and $\chi_1(E)$. For $Z(E)$ and $Z_1(E)$ we find

$$\frac{d}{d\Lambda}Z(E) = Z(E)^2\frac{d}{dE}\frac{d}{d\Lambda}\epsilon(E) \ ,$$
$$\frac{d}{d\Lambda}Z_1(E) = -iZ_1(E)^2\frac{d}{dE}\frac{d}{d\Lambda}\Gamma(E) \ . \quad \text{(A46)}$$

We insert the flow equations (A45) for $\epsilon(E)$ and $\Gamma(E)$ and neglect the derivative with respect to E of $Z_i(E)$,

$t_\alpha(E)$, and $U_\alpha(E)$ on the right-hand side, as their E-dependence is logarithmically weak. This implies $\frac{d}{dE}\chi_i(E) \simeq Z_i(E)(1 - \frac{d}{dE}\lambda_i(E)) = 1$ and hence

$$\frac{d}{d\Lambda}Z(E) =$$
$$-Z(E)^2 \left[2\pi \sum_\alpha \frac{Z_1(E - \mu_\alpha)}{(\Lambda - i\chi_1(E - \mu_\alpha))^2} U_\alpha^{(0)} t_\alpha(E - \mu_\alpha)^2 \right.,$$
$$\left. - \frac{2\Lambda Z(E)}{(\Lambda - i\chi(E))(2\Lambda - i\chi(E))} \gamma(E) \right]$$

$$\frac{d}{d\Lambda}Z_1(E) = 2\pi Z_1(E)^2 \sum_\alpha \frac{Z(E + \mu_\alpha)}{(\Lambda - i\chi(E + \mu_\alpha))^2} U_\alpha^{(0)} t_\alpha(E)^2$$
$$+ (E \to -E)^* . \qquad (A47)$$

The first terms include an additional factor t_α^2/Λ and can be neglected to leading order, yielding

$$\frac{d}{d\Lambda}Z(E) \simeq \frac{2\Lambda Z(E)^3 \gamma(E)}{(\Lambda - i\chi(E))(2\Lambda - i\chi(E))} \qquad (A48)$$

and a constant for $Z_1(E) \simeq 1$. The comparison with the equation for $U_\alpha(E)$ implies

$$Z(E)U_\alpha(E) \simeq U_\alpha^{(0)} , \qquad (A49)$$

i.e. the product $Z(E)U_\alpha(E)$ being unrenormalized. This simplifies the flow equation for $t_\alpha(E)$ in (A45) to

$$\frac{d}{d\Lambda}t_\alpha(E) = -\frac{U_\alpha^{(0)}}{\Lambda - i\chi(E + \mu_\alpha)} t_\alpha(E) . \qquad (A50)$$

We can now derive the equation for $\chi(E) = Z(E)(E - \epsilon(E))$. The above expressions yield

$$\frac{d}{d\Lambda}Z(E)\epsilon(E) =$$
$$2\pi i \sum_\alpha \frac{Z(E)}{\Lambda - i\chi_1(E - \mu_\alpha)} U_\alpha^{(0)} t_\alpha(E - \mu_\alpha)^2$$
$$-2\gamma_0 \left[i\ln\frac{2\Lambda - i\chi(E)}{\Lambda - i\chi(E)} - \frac{\Lambda Z(E)\epsilon(E)}{(2\Lambda - i\chi(E))(\Lambda - i\chi(E))} \right] ,$$
$$(A51)$$

with $\chi_1(E) = E + i\Gamma(E)$ and $\gamma_0 = \sum_\alpha (U_\alpha^{(0)})^2$. From Eq. (A48) for $Z(E)$ the equation for $\chi(E)$ reads

$$\frac{d}{d\Lambda}\chi(E) =$$
$$-2\pi i \sum_\alpha \frac{Z(E)}{\Lambda - i\chi_1(E - \mu_\alpha)} U_\alpha^{(0)} t_\alpha(E - \mu_\alpha)^2$$
$$+2\gamma_0 \left[i\ln\frac{2\Lambda - i\chi(E)}{\Lambda - i\chi(E)} + \frac{\Lambda\chi(E)}{(2\Lambda - i\chi(E))(\Lambda - i\chi(E))} \right] .$$
$$(A52)$$

In leading order, this equation can approximately be integrated by

$$\chi(E) = 2i\gamma_0\Lambda\ln\frac{2\Lambda - i\chi(E)}{\Lambda - i\chi(E)} + \chi'(E) , \quad (A53)$$

with

$$\frac{d}{d\Lambda}\chi'(E) = -2\pi i \sum_\alpha \frac{Z(E)}{\Lambda - i\chi_1(E - \mu_\alpha)} U_\alpha^{(0)} t_\alpha(E - \mu_\alpha)^2 .$$
$$(A54)$$

The terms neglected stem from the Λ-dependence of $\chi(E)$ leading to higher order terms of order $\gamma_0\frac{d}{d\Lambda}\chi(E) \sim O(U^3)$. The first term of (A54) is important since it cancels the large term proportional to D in the initial condition for $\epsilon(E)$, see (A4). To achieve this, the following relation is needed between the physical reservoir band width and the initial cutoff of the RG flow

$$\Lambda_0 = \frac{\pi^2}{16\ln 2}D . \qquad (A55)$$

Using (A4) and neglecting unimportant terms $\sim O(\gamma_0)$, the initial condition for $\chi'(E)$ then reads

$$\chi'(E)|_{\Lambda_0} = E - \epsilon_0 + i\frac{\Gamma^{(0)}}{2} . \qquad (A56)$$

The RG equation (A54) together with the initial condition (A56) lead to the RG equation (34) with the definition $\tilde{\Gamma}_\alpha(E) = 2\pi Z(E + \mu_\alpha)t_\alpha(E)^2$. Since the first term of (A53) is of order $\sim \gamma_0$ it can be neglected in all denominators of (A45) and $(\Lambda - i\chi(E))^{-1} \simeq (\Lambda - i\chi'(E))^{-1}$. Thus, the first two RG equations of (A45) are identical to the RG equations (32) and (33). Finally, one obtains the RG equation (31) for $\tilde{\Gamma}_\alpha(E)$ if one combines the RG equations (A50) for $t_\alpha(E)$ with the RG equation (A48) for $Z(E)$ and uses (A49).

Appendix B: Contour integrations for the time evolution

The evaluation of the auxiliary functions $J_\pm(t)$ defined in (96) is performed using standard techniques for contour integrations. The integrand has poles at $z = 0$ and $z = -i\tilde{\Gamma}$ as well as branch cuts starting at $z = \tilde{\epsilon} \pm V/2 - i\tilde{\Gamma}_\epsilon/2$ and $z = -\tilde{\epsilon} \pm V/2 - i\tilde{\Gamma}_\epsilon/2$, see Fig. 12.

Let us first consider the non-interacting case. The solution of RG equations yields a result for the rates Γ_α and Γ'_α, which appears to be exact in the scaling limit. In particular, for symmetric coupling we obtain $\Gamma(z) = \Gamma_L^{(0)} + \Gamma_R^{(0)} = \Gamma^{(0)} \equiv T_K$, $\Gamma_\pm(z) = \frac{1}{2}T_K \pm \sum_\alpha \Gamma'_\alpha(z)$, $\Gamma_\alpha^{1/2} = \Gamma'_\alpha \pm \frac{1}{4}T_K$, and

$$\Gamma'_\alpha(z) = \frac{iT_K}{4\pi}\left[\ln\left(\frac{T_K}{2} - i(z + \mu_\alpha - \epsilon_0)\right)\right.$$
$$\left. - \ln\left(\frac{T_K}{2} - i(z - \mu_\alpha + \epsilon_0)\right)\right]. \quad (B1)$$

Using these values we obtain (109) and (110) from (95) and (97), respectively, where the functions $F_{0/1,\alpha}(t)$ are
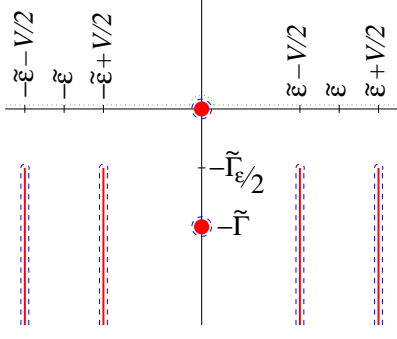
FIG. 12. (Color online) Analytic structure of the integrand of $J_\pm(t)$. All singularities appear in the lower half plane. Red dots stand for poles while red solid lines represent branch cuts. The pole at $z = 0$ corresponds to the stationary state. The blue dashed and green dotted lines are the original and deformed integration contours respectively.

originally defined by

$$F_{0/1,\alpha}(t) = \frac{i}{2\pi T_K} \int_{-\infty+i0^+}^{\infty+i0^+} dz e^{-izt} \frac{\Gamma'_\alpha(z)}{z + i\frac{T_K}{2} \mp i\frac{T_K}{2}} . \quad (B2)$$

We note their important property

$$\frac{d}{dt}[F_{0,\alpha}(t) - F_{1,\alpha}(t)] = T_K F_{1,\alpha}(t) , \quad (B3)$$

which guarantees the current conservation $\frac{d}{dt}n(t) = \sum_\gamma I_\gamma(t)$.

Let us now show that the result of integration in (B2) leads to Eq. (111). To this end we deform the contour of integration from the real axis to the paths embracing the poles and the branch cuts shown in the Fig. 12. The positions of the nonzero pole as well as of the branch points of $\Gamma'_\alpha(z)$ (see Eq. (B1) above) in the integrand of (B2) are given by the bare values of $\tilde\Gamma = \tilde\Gamma_\epsilon = T_K$ and $\tilde\epsilon = \epsilon_0$. We obtain the following contributions to $F_{0/1,\alpha}(t) = F_{0/1,\alpha}^p(t) + F_{0/1,\alpha}^{br.c.}(t)$. The pole contribution equals

$$F_{0,\alpha}^p(t) = \frac{\Gamma'_\alpha(0)}{T_K}, \quad F_{1,\alpha}^p(t) = \frac{\Gamma'_\alpha(-iT_K)}{T_K}e^{-T_K t}, \quad (B4)$$

where

$$\Gamma'_\alpha(0) = -\Gamma'_\alpha(-iT_K) = \frac{T_K}{2\pi}\arctan\frac{\mu_\alpha - \epsilon_0}{T_K/2}. \quad (B5)$$

The branch-cut contribution equals

$$F_{0/1,\alpha}^{br.c.}(t) = \frac{ie^{i(\epsilon_0-\mu_\alpha)t}}{2\pi T_K} \int_{-i\infty}^{-i\frac{T_K}{2}} \frac{d(iy)e^{yt}}{iy + i\frac{T_K}{2} \mp i\frac{T_K}{2} - (\epsilon_0 - \mu_\alpha)}$$
$$\times \frac{iT_K}{4\pi}(-2\pi i) - (\epsilon_0 - \mu_\alpha \to -\epsilon_0 + \mu_\alpha)$$
$$= -\mathrm{Im}\frac{e^{i(\epsilon_0-\mu_\alpha)t-\frac{T_K t}{2}}}{2\pi}\int_{-\infty}^0 \frac{dy\, e^{yt}}{y \mp \frac{T_K}{2} + i(\epsilon_0 - \mu_\alpha)}$$
$$= \mathrm{Im}\frac{e^{i(\epsilon_0-\mu_\alpha)t-\frac{T_K t}{2}}}{2\pi}\int_0^\infty \frac{dx\, e^{-x}}{x \pm \frac{T_K t}{2} - i(\epsilon_0 - \mu_\alpha)t}$$
$$= -\frac{e^{-T_K t/2 \pm T_K t/2}}{2\pi}\mathrm{Im\,Ei}\left(\mp\frac{T_K t}{2} + i(\epsilon_0 - \mu_\alpha)t\right),$$
$$(B6)$$

where we exploit the analytic continuation of the exponential integral function (see 8.212.5 of Ref. 36 and Ref. 37)

$$\mathrm{Ei}(\pm z) = -e^{\pm z}\int_0^\infty \frac{e^{-x}}{x \mp z}dx, \quad (\mathrm{Re}\, z > 0). \quad (B7)$$

Combining (B4), (B5) and (B6) we obtain the formula (111). We also note that

$$F_{0/1,\alpha}^{br.c.}(t = 0^+) = -\frac{1}{2\pi}\mathrm{Im}\int_{-\infty}^0 \frac{dy}{y \mp \frac{T_K}{2} + i(\epsilon_0 - \mu_\alpha)}$$
$$= \pm\frac{1}{2\pi}\arctan\frac{\epsilon_0 - \mu_\alpha}{T_K/2}, \quad (B8)$$

which implies the property

$$F_{0/1,\alpha}(t = 0^+) = 0. \quad (B9)$$

In the interacting case, the analytic structure remain very similar to that of the non-inteacting case. The main difference is contained in the type of branching behavior which changes from the logarithmic to the power-law one. Additionally, positions of the branch point as well as a position of the nonzero pole are shifted to interaction-dependent values.

For $|\tilde\epsilon - V/2| \gg T_K$ we can treat all poles and branch cuts separately. Thus the evaluation of $J_\pm(t)$ boils down to

$$J_\pm(t) = -\frac{1}{2} \mp \frac{\Gamma'(0)}{\Gamma(0)} \quad (B10)$$
$$+ \left(\frac{1}{2} \pm \frac{\Gamma'(-i\tilde\Gamma)}{\tilde\Gamma}\right)e^{-\tilde\Gamma t}\mathrm{Res}\left(\frac{1}{z + i\Gamma(z)}, z = -i\tilde\Gamma\right)$$
$$+ \frac{i}{2\pi}\sum_{\alpha=\pm V/2}\sum_{\beta=\pm\tilde\epsilon} e^{-i(\alpha+\beta)t}\int_{-\infty}^{-\tilde\Gamma_\epsilon/2} \frac{dy\, e^{yt}}{\alpha + \beta + iy}$$
$$\times\left(\frac{\Gamma_\pm(\alpha + \beta - \eta + iy)}{\alpha + \beta + iy + i\Gamma(\alpha + \beta - \eta + iy)} - (\eta \to -\eta)\right) .$$

Using $\Gamma_\pm(z) = \frac{1}{2}\Gamma(z) \pm \Gamma'(z)$ it can be cast in the form

$$J_\pm(t) = -\frac{1}{2} \mp \frac{\Gamma'(0)}{\Gamma(0)} \tag{B11}$$

$$+ \left(\frac{1}{2} \pm \frac{\Gamma'(-i\tilde{\Gamma})}{\tilde{\Gamma}}\right) e^{-\tilde{\Gamma}t} + J_b(t) \pm J_b'(t) \,,$$

where the first two terms equal n^{st}. Then a straightforward calculation yields

$$J_b(t) = \frac{2\sin(\pi g)}{\pi} \frac{e^{-\frac{\tilde{\Gamma}_\epsilon}{2}t}}{(tT_K)^{1+g}} \sum_{\alpha=\pm V/2} \sum_{\beta=\pm\tilde{\epsilon}} e^{-i(\alpha+\beta)t} \tag{B12}$$

$$\times \int_0^\infty \frac{ds}{s^g} \frac{e^{-s}}{\left[4\frac{(\alpha+\beta-i\tilde{\Gamma}_\epsilon/2)t-is}{(tT_K)^{1+g}} + \frac{i}{(-s-2i\alpha t)^g} + \frac{i}{(-s-2i\beta t)^g} + \frac{i}{(-s-2i(\alpha+\beta)t)^g} + \frac{i}{s^g}\cos(\pi g)\right]^2 + \frac{\sin^2(\pi g)}{s^{2g}}} \,,$$

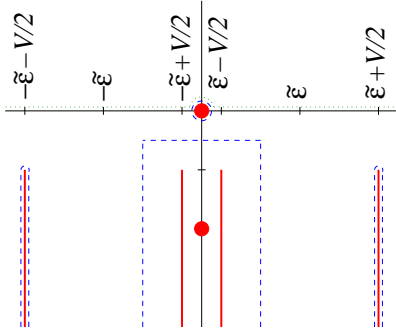
FIG. 13. (Color online) Integration contour for $J_\pm(t)$ on resonance $|\tilde{\epsilon} - V/2| \ll T_K$.

while $J_b'(t)$ has been evaluated numerically. We note that the factor $\beta/\tilde{\epsilon}$ just gives a sign. For $V, |\tilde{\epsilon}-V/2| \gg T_K, 1/t$ we obtain (106). Close to resonance, $|\tilde{\epsilon}-V/2| \ll T_K$, the two branch cuts starting at $z = \pm\tilde{\epsilon}\mp V/2 - i\tilde{\Gamma}_\epsilon/2$ are very close to the pole at $z = -i\tilde{\Gamma}$, which leads to a numerical instability in the calculation of its residue. Therefore, it is advantageous to directly evaluate $J_\pm(t)$ as defined in (96) on the contour shown in Fig. 13, thereby encircling the pole at $z = -i\tilde{\Gamma}$.

The time evolution of the current given in (97) can be cast in the form

$$I_L(t) = J^1(t) + \left(\frac{1}{2} - n(0)\right) J^2(t) + J^3(t) \,, \tag{B13}$$

where

$$J^1(t) = \frac{i}{2\pi} \int_{-\infty+i0^+}^{\infty+i0^+} \frac{dz}{z} \Gamma_L'(z) e^{-izt} \,, \tag{B14}$$

$$J^2(t) = \frac{i}{2\pi} \int_{-\infty+i0^+}^{\infty+i0^+} \frac{dz}{z+i\Gamma(z)} \Gamma_L(z) e^{-izt} \,, \tag{B15}$$

$$J^3(t) = \frac{1}{2\pi} \int_{-\infty+i0^+}^{\infty+i0^+} \frac{dz}{z} \frac{\Gamma'(z)\,\Gamma_L(z)}{z+i\Gamma(z)} e^{-izt} \,. \tag{B16}$$

The evaluation is analogous to the one for $J_\pm(t)$ above. In particular, in the long-time limit $Vt, |\tilde{\epsilon} - V/2|t \gg 1$ off resonance we find

$$J^1(t) = \Gamma_L'(z=0) + \frac{T_K}{2\pi}(T_K t)^g e^{-\tilde{\Gamma}_\epsilon t/2} \frac{\cos\big((\tilde{\epsilon}-V/2)t\big)}{(\tilde{\epsilon}-V/2)t} \,,$$

$$J^2(t) = \Gamma_L(-i\tilde{\Gamma}) e^{-i\tilde{\Gamma}t} \,,$$

$$J^3(t) = -\frac{\Gamma'(0)}{\Gamma(0)}\Gamma_L(0) + \frac{\Gamma'(-i\tilde{\Gamma})}{\tilde{\Gamma}}\Gamma_L(-i\tilde{\Gamma}) e^{-i\tilde{\Gamma}t} \,, \tag{B17}$$

where for J^2 and J^3 terms in $O(U^{(0)})$ were neglected. The first terms in J^1 and J^3 together yield the stationary current (53).

[1] P.B. Vigman and A.M. Finkel'shtein, Sov. Phys. JETP **48**, 102 (1978).

[2] P. Schlottmann, J. Magn. magn. Mater. **7**, 72 (1978); J. Phys. (Paris) **39**, C6-1486 (1978).

[3] P.W. Anderson and G. Yuval, Phys. Rev. Lett. **23**, 89 (1969); G. Yuval and P.W. Anderson, Phys. Rev. B **1**, 1522 (1970); P.W. Anderson, G. Yuval, and D.R. Hamann, Phys. Rev. B **1**, 4464 (1970); K.D. Schotte, Z. Physik **230**, 99 (1970).

[4] G. Toulouse, C. R. Acad. Sci. (Paris) **268**, 1200 (1969).

[5] V.M. Filyov and P.B. Wiegmann, Phys. Lett. A **76**, 283 (1980); A.M. Tsvelick and P.B. Wiegmann, Adv. Phys. **32**,

453 (1983).

[6] P. Schlottmann, Phys. Rev. B **25**, 4815 (1982); *ibid.* **25**, 4828 (1982); *ibid.* **25**, 4838 (1982).

[7] A.O. Gogolin, A.A. Nersesyan, and A.M. Tsvelik, *Bosonization and Strongly Correlated Systems* (Cambridge University Press, Cambridge, 2004).

[8] P. Mehta and N. Andrei, Phys. Rev. Lett. **96**, 216802 (2006); P. Mehta, S.-P. Chao, and N. Andrei, arXiv:cond-mat/0703426.

[9] B. Doyon, Phys. Rev. Lett. **99**, 076806 (2007).

[10] A. Golub, Phys. Rev. B **76**, 193307 (2007).

[11] A. Nishino and N. Hatano, J. Phys. Soc. Jpn. **76**, 063002 (2007).

[12] A. Nishino, T. Imamura, and N. Hatano, Phys. Rev. Lett. **102**, 146803 (2009).

[13] E. Boulat and H. Saleur, Phys. Rev. B **77**, 033409 (2008).

[14] E. Boulat, H. Saleur, and P. Schmitteckert, Phys. Rev. Lett. **101**, 140601 (2008).

[15] A. Branschädel, E. Boulat, H. Saleur, and P. Schmitteckert, Phys. Rev. Lett. **105**, 146805 (2010).

[16] L. Borda, K. Vladár, and A. Zawadowski, Phys. Rev. B **75**, 125107 (2007); L. Borda, A. Schiller, and A. Zawadowski, Phys. Rev. B **78**, 201301(R) (2008).

[17] C. Karrasch, M. Pletyukhov, L. Borda, and V. Meden, Phys. Rev. B **81**, 125122 (2010).

[18] C. Karrasch, S. Andergassen, M. Pletyukhov, D. Schuricht, L. Borda, V. Meden, and H. Schoeller, Europhys. Lett. **90**, 30003 (2010).

[19] S.G. Jakobs, V. Meden, and H. Schoeller, Phys. Rev. Lett. **99**, 150603 (2007); S.G. Jakobs, M. Pletyukhov, and H. Schoeller, Phys. Rev. B **81**, 195109 (2010). R. Gezzi, Th. Pruschke, and V. Meden, Phys. Rev. B **75**, 045324 (2007).

[20] H. Schoeller, Eur. Phys. J. Special Topics **168**, 179 (2009).

[21] S. Andergassen, V. Meden, H. Schoeller, J. Splettstoesser, and M.R. Wegewijs, Nanotechnology **21**, 272001 (2010).

[22] H. Schoeller and F. Reininghaus, Phys. Rev. B **80**, 045117 (2009); *ibid.* Phys. Rev. B **80**, 209901(E) (2009); D. Schuricht and H. Schoeller, Phys. Rev. B **80**, 075120 (2009).

[23] M. Pletyukhov, D. Schuricht, and H. Schoeller, Phys. Rev. Lett. **104**, 106801 (2010).

[24] B. Doyon and N. Andrei, Phys. Rev. B **73**, 245326 (2006).

[25] S. Kehrein, Phys. Rev. Lett. **95**, 056602 (2005); S. Kehrein, *The Flow Equation Approach to Many-Particle Systems* (Springer, Berlin, 2006); P. Fritsch and S. Kehrein, Ann. Phys. **324**, 1105 (2009); P. Fritsch and S. Kehrein, Phys. Rev. B **81**, 035113 (2010).

[26] L. Borda and A. Zawadowski, Phys. Rev. B **81**, 153303 (2010).

[27] This corrects a typographical error in Eq. (8) of Ref. 18.

[28] J. Peskill, in *Introduction to Quantum Computation and Information* (H.-K. Lo, S. Popescu, and T. Spiller, World Scientific, Singapore, 1998); D.P. DiVincenzo and D. Loss, Phys. Rev. B **71**, 035318 (2005); J. Fischer and D. Loss, Science **324**, 1277 (2009).

[29] M. Büttiker, A. Prêtre, and H. Thomas, Phys. Rev. Lett. **70**, 4114 (1993); J. Fransson, O. Eriksson, and I. Sandalov, Phys. Rev. B **66**, 195319 (2002).

[30] T.L. Schmidt, P. Werner, L. Mühlbacher, and A. Komnik, Phys. Rev. B **78**, 235110 (2008).

[31] A.J. Leggett, S. Chakravarty, A.T. Dorsey, M.P.A. Fisher, A. Garg, and W. Zwerger, Rev. Mod. Phys. **59**, 1 (1987).

[32] F. Lesage and H. Saleur, Phys. Rev. Lett. **80**, 4370 (1998).

[33] F.B. Anders and A. Schiller, Phys. Rev. Lett. **95**, 196801 (2005); Phys. Rev. B **74**, 245113 (2006).

[34] A. Komnik, Phys. Rev. B **79**, 245102 (2009).

[35] D. Lobaskin and S. Kehrein, Phys. Rev. B **71**, 193303 (2005); D. Lobaskin and S. Kehrein, J. Stat. Phys. **123**, 301 (2006); M. Heyl and S. Kehrein, J. Phys.: Condens. Matter **22**, 345604 (2010).

[36] I.S. Gradshteyn and I.M. Ryzhik, *Table of Integrals, Series, and Products* (Academic Press, London, 1994).

[37] M. Abramowitz and I.A. Stegun, *Handbook of Mathematical Functions* (Dover, New York, 1965).